101

Journal of Mathematical Biology 1, 187—225 (1975)

A Mathematical Model of Neutrophil Production and Control in Normal Man

S. I. Rubinow and **J. L. Lebowitz***, New York

Received July 2, 1973; revised May 23, 1974

Summary

A comprehensive mathematical model of neutrophil production in normal man is presented. The model incorporates three control elements which regulate homeostatically the rates of release of marrow cells to proliferation, maturation, and to the blood. The steady state properties of the model are demonstrated analytically. The basic equations of the model, which are nonlinear, have been integrated numerically. The solutions so obtained display graphically the dynamical response of the system to various perturbations, which simulate experimental investigations that have been made in the past of granulocytopoiesis. By an appropriate choice of values of the parameters characterizing the system, it is shown how most of the principal kinetic properties of the neutrophil production and control system are represented in a quantitative manner.

1. Introduction

The introduction of radioactive tracers as cell labels has led, inter alia, to a rapid accumulation of knowledge during the past 20 years or so of the kinetic behavior of the neutrophil and its precursors in the blood and marrow of man. Many investigations, too numerous to mention here, have contributed to this knowledge, and several excellent reviews of this subject may be found in the literature [1, 2, 3, 4]. The process of production of neutrophils is rather complicated, and many details of the process are as yet unknown. However, a fairly good qualitative or semi-quantitative description of the life history of the neutrophil exists. Concomitant with the study of particular aspects of this life history, there have been a number of attempts to describe such aspects theoretically in quantitative terms. Examples of mathematical models of this nature are those related to the distribution in number of neutrophil precursors in the marrow [5], the blood-granulocyte-specific-activity curve which follows the labeling of all neutrophils and their precursors [6], and the homeostatic regulation of blood neutrophil levels [7]. However, up to the present time, there does not exist a single comprehensive quantitative model representing both the steady state and

* Also Physics Department, Belfer Graduate School of Sciences, Yeshiva University, New York, NY 10019, U.S.A.

the dynamical behavior of the neutrophil production system. By dynamical behavior, we mean the response of the production system to perturbations.

The purpose of the present work is to propose such a comprehensive mathematical model of the natural history of the neutrophil and its precursors which will simulate, more or less, all of the known kinetic aspects of this history. In developing our model, we make many idealized assumptions. These are made for the most part in the interest of simplicity, and because of the lack of quantified data. However, sometimes, as in the representation of the proliferative precursors of the mature neutrophil, we are forced to simplify the model because the data is not consistent with any simple proliferative scheme. Nevertheless, we believe that these simplifications do not invalidate the general utility of our model.

We first review, in section 2, the known quantified facts of granulocytopoiesis. Because the neutrophil is the most common granulocyte, the terms neutrophil and granulocyte are often used interchangeably in the literature, and we shall do so here. In section 3 we describe our model, which consists of five compartments, two, proliferative, and three, nonproliferative. Associated with each compartment is a partial differential equation for the cell density function, which describes the population in the compartment as a function of the variables age (or maturity) and time. The model also contains three feedback control elements which regulate homeostatically the rate of release of cells from the marrow to the blood, the rate of production, and the rate of release to maturation of cells in the proliferative pool.

Because of the control elements in the model, the model equations are nonlinear, and therefore cannot be solved in an analytic manner, in general. However, the steady state solution can be found, as shown in section 4. The steady state solution is useful for deducing many properties of the system, and is utilized in section 6, in conjunction with the known experimental facts, to determine the values of seven of the parameters. These seven parameters characterize the steady state behavior of the system.

A partial integration of the model equations can be achieved, so as to reduce the equation system to ordinary differential equations. This reduction is demonstrated in section 5. Numerical solutions of these equations, performed on a computer, which yield the populations in the compartments as functions of the time, following a given disturbance of the system, are displayed in section 7. A comparison of these solutions is made with the known semiquantitative behavior of the neutrophil production system, following a disturbance. This comparison provides information concerning the dynamical parameters of the system. The latter parameters serve to determine the dynamical response of the system to perturbations of the steady state cell populations.

We find that our model, although it oversimplifies certain essential details of the neutrophil production scheme, can be made to successfully simulate the significant quantitative details of granulocytopoiesis. The model forms the basis of a mathematical representative of the natural kinetic history of the leukemic state, which will be presented in a subsequent work.

2. Granulocytopoiesis

We shall present a succinct summary of most of the known facts about neutrophil production and control in a normal man. The entire production scheme is schematically illustrated in Fig. 1. There is believed to exist in the marrow a

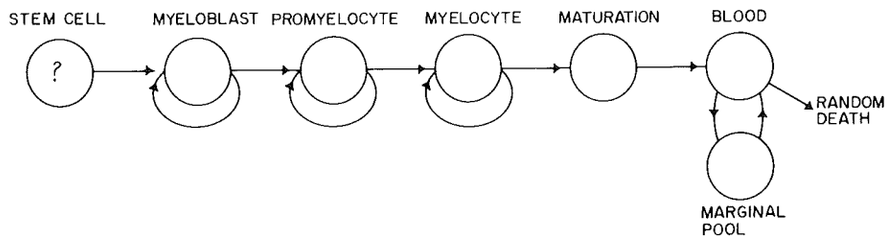

Fig. 1. The normal neutrophil production scheme is schematically illustrated. The stem cell has not been identified, although it is usually assumed to exist. The myeloblast, promyelocyte, and myelocyte are proliferative. The maturation compartment consists of metamyelocytes, band forms, and segmented neutrophils, all nonproliferative

stem cell from which all granulocytes found in the blood are derived. Indirect evidence for its existence comes from observations indicating that abnormally large production of one type of blood cell leads to a concurrent decrease in production of the other types [8, 9]. Further evidence comes from the observation that spleen colonies derived from irradiated mice, and presumably arising from a single precursor cell, sometimes contain erythroid, granulocytic, and megakaryocytic cells [10]. The identification of the stem cell in the marrow has yet to be made. Recent evidence suggests that a lymphocyte-like cell functions as the stem cell [11].

The earliest cytologically identifiable neutrophil precursor normally found in the bone marrow is the myeloblast. The myeloblast is a proliferative cell, and perhaps functions as an additional stem cell for the production of granulocytes only. It most likely produces the promyelocyte [12], likewise a proliferative cell. The promyelocyte in turn most likely produces the myelocyte, which is the most abundant proliferative neutrophil precursor found in the marrow. Myelocytes give rise to a maturing and nonproliferating pool of precursor cells. These cells are cytologically and morphologically distinguishable, in the order of their maturation, as metamyelocytes, band forms, and segmented neutrophils. A certain portion, perhaps one half, of the more mature nonproliferating granulocytes constitute a "mature granulocyte reserve" compartment of the bone marrow. From here, they are released into the blood by an unknown mechanism.

When granulocytes are taken from a donor's blood, labeled with DFP^{32}, and transfused back again, only 50% of the labeled cells can be accounted for in the circulating blood [13]. This has been interpreted to mean that the total blood granulocyte pool consists of two subcompartments, a circulating granulocyte compartment and a marginal granulocyte compartment, which contain approximately equal numbers of cells, and which equilibrate rapidly with each other.

Granulocytes have been observed adhering to walls of blood vessels, and such cells are presumed to be part of the marginal granulocyte compartment. The cells in the marginal compartment are rapidly mobilized to join the circulating compartment by means of exercise or the injection of adrenaline into the blood. From the observed rate of disappearance of labeled cells from the blood, it has been determined that the granulocyte loss from the blood is a random process, and that the half-time for granulocyte disappearance from the blood is 6.7 hours [14]. Only a negligible number of cells are presumed to die because of senescence, as deduced by the scarcity of pyknotic cells in the blood [15].

In a normal marrow, the relative number of cells of each type that have been observed by different investigators is somewhat variable, as shown in Table 1. In this table, the relative numbers are reported relative to the observed number of myelocytes, which has been set equal to unity. It can be seen that the myeloblast, the earliest and least common granulocyte precursor, is subject to the greatest variation in observed number, followed by the promyelocyte. Even the ratio of non-proliferative to proliferative cells, calculated in the last column in Table 1, has a range of variation extending from 1.27 to 7.57. There is some belief that this ratio is approximately 3 [16].

Based on the labeling of proliferating cells in *S*-phase with tritiated thymidine, the mean time of *S*-phase, or DNA synthesis time of proliferating cells has been estimated to be 13.5 hr [17] or 16 hr [18]. The earliest transit time for myelocytes labeled in *S*-phase to appear as metamyelocytes is 3 hr [19].

The data on mitotic indices of the proliferative cells is shown in Table 2. The preponderance of investigators find a mean mitotic index in the proliferative pool of approximately 1%. The mean generation time of all the proliferating cells is approximately 48 hr based on the decay of intensity of radioactively labeled cells [19], and based on mitotic indices and relative numbers of cell

Table 1. *Relative Number of Marrow Granulocytes in Normal Man. Normalization: Myelocyte Number = 1*

Proliferative Cells			Nonproliferative Cells			Ratio of Non-proliferative Cells to Proliferative Cells	Source
Myelo-blast	Pro-myelo-cyte	Myelo-cyte	Meta-myelo cyte	Band	Se-gment-ed		
0.10	0.33	1	1.55	5.71	3.57	7.57	Osgood & Seaman [47]
0.15		1	0.99	2.69	2.08	5.01	Vaughan & Brockmyre [48]
0.16	0.43	1	1.28	2.28	1.90	3.43	Miale [49]
0.17	0.42	1	1.83			2.20	Wintrobe [50]
0.07*	0.26*	1	1.04	1.38	0.96	2.54	Donohue et al. [26]; Athens [51]*
0.06	0.07	1	0.45	0.50	0.49	1.27	Lala et al. [52]
0.06	0.21	1				1.74	Killman et al. [53]
0.11	0.23	1					Rondanelli et al. [54]
0.02	0.06	1	0.92	1.63	1.67	3.91	Cronkite et al. [55]
0.02	0.06	1	0.80	1.32	1.90	3.72	Cronkite & Vincent [3]

types in the marrow [20, 5]. The interdivision time of myelocytes observed in vitro is approximately 30 hr [21].

Generation times can also be inferred from the labeling index (L. I.), the fraction of proliferative cells which are radioactively labeled following a pulse exposure to tritiated thymidine. Most of the available data regarding labeling indices is summarized in Table 3. However, as will be shown in the appendix, the inferences regarding the mean generation times of the myeloblast, promyelocyte, and myelocyte that are inferred from the relative marrow counts combined with the labeling index data are decidedly not in agreement with the estimates of these times that are inferred from the relative marrow counts when combined with the mitotic index data.

Table 2. *Observed Miotic Indices of Marrow Proliferative Cells in Normal Man*

Myeloblast	Pro-myelocyte	Myelocyte	Mean Mitatic Index of Proliferative Cells	Source
0.11	0.11	0.052	0.059	Lala et al. [52]
0.025	0.015	0.011	0.012	Killman et al. [53]
0.0236	0.0133	0.0079	0.010	Rondanelli et al. [54]
			0.008*	Videbaek [56]
			0.0077*	Begemann & Hemmerle [57]
			0.011	Boll & Ganssen [58]

* Promyelocytes and Myelocytes only.

Table 3. *Initial Labeling Index of Marrow Proliferative Cells in Normal Man*

Myeloblast	Pro-myelocyte	Myelocyte	Mean Labeling Index of Proliferative Cells	Source
0.85	0.65	0.23	0.27	Cronkite et al. [55]
0.15	0.59	0.22	0.24	Cronkite & Vincent [3]
	0.32*	0.25*	0.28*	Lundmark [59]
0.46	0.45	0.13		Gavosto [60]
0.69	0.58	0.32		Mauri et al. [61]
0.65		0.20		Kuroyanai & Saito [62]
0.40—0.50†	0.40—0.50†	0.15—0.20		Mauri [63]
			0.35—0.38	Lin & Bouroncle [64]
0.50				Alfrey et al. [65]
		0.35		Schmid et al. [66]
0.63		0.38		Ogawa [67]

* Infants and children.

† Myeloblasts and promyelocytes combined.

When proliferating cells are exposed to pulse labeling with tritiated thymidine, labeled cells appear in the blood four days later [22] (see Fig. 2). This has been interpreted to mean that there is a minimum obligatory transit time of proliferating cells through the metamyelocyte and band compartments [3], with a

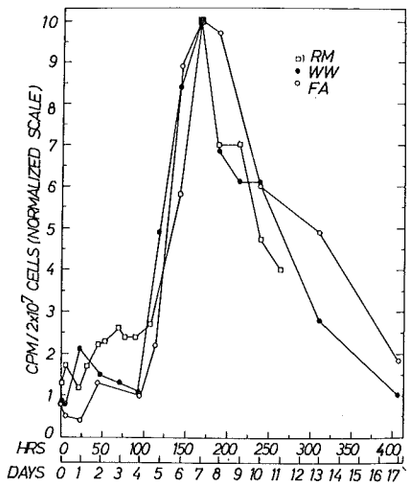

Fig. 2. The appearance of labeled granulocytes in the blood in three normal individuals, following the administration of tritiated thymidine on day 0, from Perry et al. [22]

magnitude of approximately 4 days. The segmented neutrophils and some of the band cells in the marrow are believed to constitute the marrow reserve compartment, but estimates of the number of cells in this compartment are very variable. Perhaps the best quantitative information regarding it is contained in the blood-granulocyte-specific-activity (BGSA) curves [23] (see Fig. 3), obtained by measuring the radioactivity of granulocytes in the blood following the intravenous administration of the radioactive label DFP^{32}. The latter substance

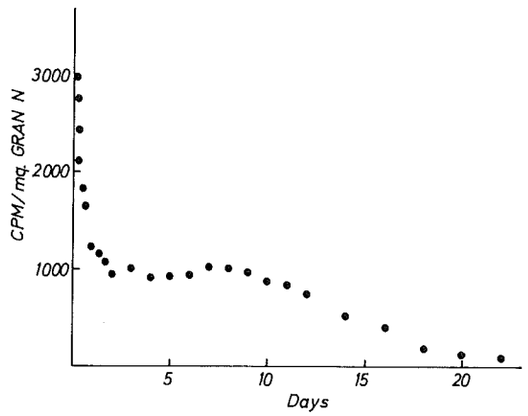

Fig. 3. The blood-granulocyte-serum-activity curve following labeling of all granulocytes and their precursors at time zero with DFP^{32}. The experimental points shown represent the mean data for 18 subjects, from Warner & Athens [6]

labels all myelocytes, nonproliferative marrow precursors, and cells in the blood, with the relative labeling values 1, 2, and 4, respectively. Based on a mathematical model of granulocyte production, the mean time in 21 normal subjects for a myelocyte to divide, mature, and enter the blood was inferred to be 11.4 days [6]. Contrariwise, on the basis of tritiated thymidine pulse labeling investigations as illustrated in Fig. 2, it has been estimated that the mean transit time of granulocyte precursors through the marrow following the DNA synthesis phase is 8.5 days [24] and 6.3 days [25].

The mean number of granulocytes in the blood of a normal 70 kgm man is found to be $4.555/mm^3$ [23]. Assuming a mean blood volume of 4.76 liters, it is inferred that the mean number of blood granulocytes is $2.17 \cdot 10^{10}$ cells in a normal man, or $3.1 \cdot 10^8$ cells/kgm of body weight. The number of cells in the marginal granulocytic compartment is $3.9 \cdot 10^8$ cells/kgm [23]. Based on the latter two values, the number of cells in the total blood granulocyte compartment which is the sum of the circulating granulocyte compartment and the marginal granulocytic compartment is $4.9 \cdot 10^{10}$ cells, in a normal 70 kgm man. The total number of granulocytes in the body, inferred from measurements of iron uptake in erythrocyte precursors, was found to be $1.14 \cdot 10^{10}$/kgm [26], or $0.80 \cdot 10^{12}$ cells in a normal 70-kgm man.

The dynamical response of the granulocyte production system to perturbations has been studied in a number of different ways. Ordinarily, the steady state behavior of the system requires that the production rate equals the disappearance rate, and also equals the rate of release of cells from the marrow. In leukopheresis, granulocytes are removed from the blood artificially over a short span of time. Following such an acute depletion of the neutrophil blood count in dog or man, referred to as a state of neutropenia (or alternatively as granulocytopenia or leukopenia), neutrophils rapidly enter the blood from the marrow and produce an abnormally large number of neutrophils in the blood, or a state of neutrophilia [27—30]. The magnitude of the white blood count seen in such a state is about 2—3 times normal. The time it

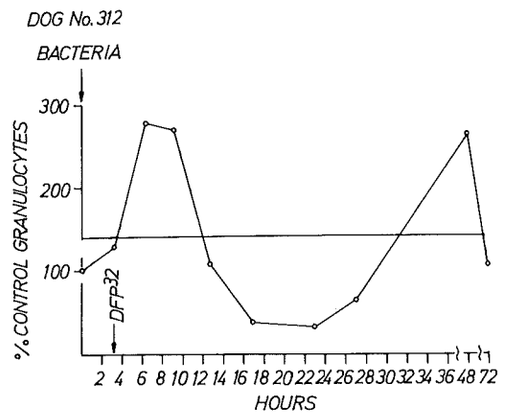

Fig. 4. The granulocyte count in the blood of the dog following induced pneumococcal pneumonia. The solid line represents the normal granulocyte count, from Marsh et al. [34]

takes for the blood to become neutrophilic following leukopheresis is a few hours. A leukocyte inducing factor (LIF) has been detected in rats which causes the release of granulocytes from the marrow to the blood [31]. Such a humoral

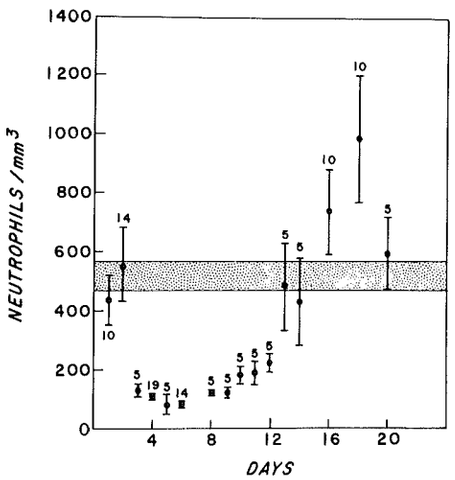

Fig. 5. The change in the mean neutrophil count in mice following total body irradiation with the hindlimb shielded. Each point represents the mean of a group of mice. The shaded area represents the mean neutrophil count in a control group. From Morley & Stohlman [39]

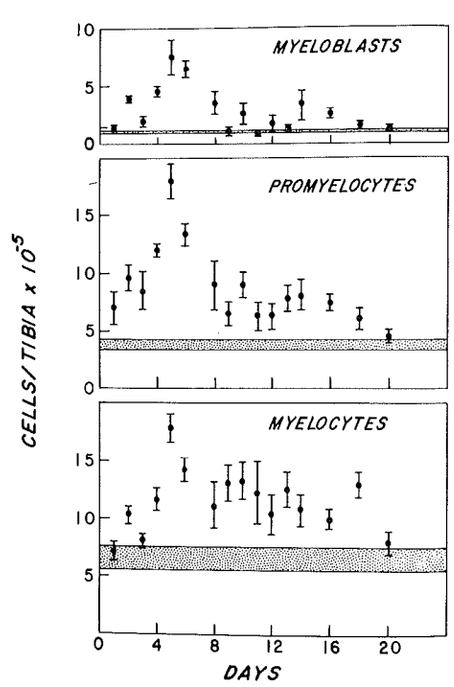

Fig. 6. The mean levels of myeloblasts, promyelocytes, and myelocytes in the shielded marrow of mice following total body irradiation, from reference [39]

factor is a suggested mechanism for regulating the release of marrow granulocytes in response to the number of granulocytes circulating in the blood [32, 33].

Speaking qualitatively, the same kind of neutrophilia observed in response to leukopheresis has been observed as a response to other stresses such as infection [34—36], bacterial endotoxin [13], and administration of adrenal corticosteroids [14, 30] or etiocholanolone [37]. An interesting feature of the response to infection in dogs, shown in Fig. 4, which has not been reported in the response to leukopheresis, is the oscillating nature of the leukocyte count.

Another means of strongly perturbing the blood cell production system has been x-irradiation. Red blood cells recover rapidly and attain a state of "overproduction" following such a stress [38]. Total body x-irradiation of mice with a shielded hindlimb was performed, in order to be able to study the response to such stress in the shielded marrow [39]. Presumably, any changes seen there are a consequence of the induced neutropenia and not the direct consequence of marrow irradiation. The irradiation destroys a majority of the neutrophils and their precursors in the body. The results of such studies are illustrated by Figs. 5 to 7. Fig. 5 shows the time course of the concentration of neutrophils in the blood for a period of 20 days following the total body irradiation. The figure shows that the concentration is below normal for about 12 days following irradiation, when it returns to normal and then "overshoots" the normal range. During the neutropenic interval in the

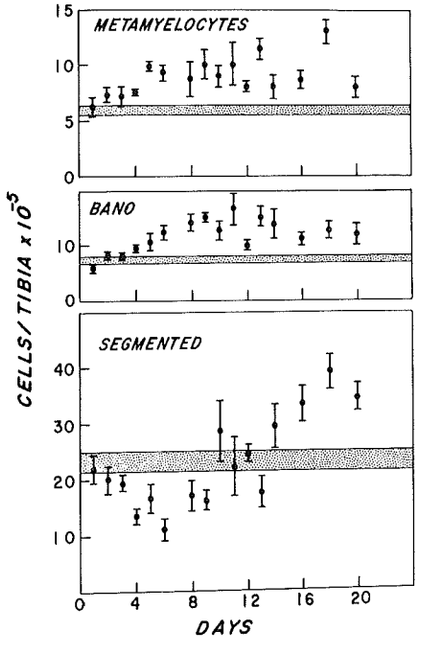

Fig. 7. The mean levels of nonproliferative cells of the marrow in the shielded marrow of mice following total body irradiation, from reference [39]

blood and following it, the concentration of proliferative cells in the marrow (of the shielded limb) is shown in Fig. 6. The concentration of younger nonproliferative cells, such as the metamyelocytes and band cells, also is higher than normal during the entire course of the experiment, as shown in Fig. 7. However, the concentration of segmented neutrophils in the marrow, initially below normal, subsequently overshoots to a large abnormal value. This overshoot anticipates the overshoot seen in the blood by several says.

The results of such x-ray studies provide qualitative evidence of the homeostatic control of the total neutrophil population in the body, and show how the neutrophil production system attempts to maintain the blood population constant at a desired level, in two ways. It does so first, by regulating the number of mature cells sent from the marrow to the blood, and second, by increasing the production of new cells, when neutropenia develops. Furthermore, the serum of mice following irradiation display an enhanced ability to stimulate the growth of granulocytic colonies in vitro [40]. This relationship has been interpreted to indicate the existence of a humoral factor, a "granulopoietin", which regulates granulocyte production.

Many investigators have sought for the mechanism by which granulocyte production is regulated. A notable recent proposal is that mature granulocytes contain and produce a feedback inhibitor of cell production, a granulocytic chalone [41]. There is some evidence that an anti-chalone is also made which regulates granulocyte production [41].

A phenomenon that relates to the existence of a granulocytic production regulator is the relatively infrequent observation of a cyclic fluctuation in the granulocyte

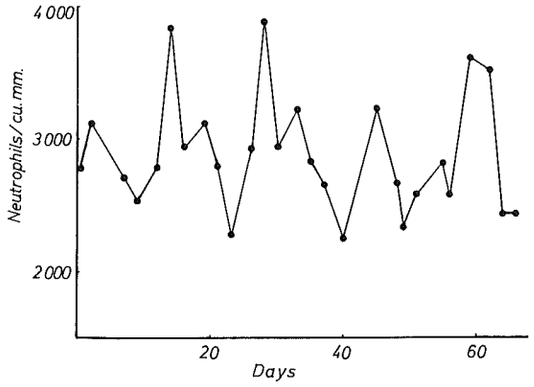

Fig. 8. Cyclic variation of the neutrophil of the neutrophil count seen in a normal individual, from the work of Morley [42]. The appearance of periodicity is not borne out by an objective statistical test (personal communication, David W. Alling)

count of normal individuals [42, 43]. Such oscillations were originally reported as occuring in eight out of eleven individuals [42] (see Fig. 8), with periods varying between 14 and 23 days, but reexamination of the data has reduced the claim to two individuals [43]. A more recent examination of eight normal individuals and two patients with Wegener's granulomatosis who were receiving cyclo-

phosphamide revealed periodic variation in only one subject, one of the two patients [43]. The period was estimated to be 5.7 days. It has been suggested, on the basis of a computer model simulating granulopoiesis, that this periodic behavior is a manifestation of feedback-control in the granulopoietic system [44]. Similar cyclic oscillations have been observed in patients with chronic granulocytic leukemia [45], and in some cases of cyclic neutropenia [46].

3. Model of Neutrophil Production

The presumed mode or sequence of development of mature neutrophils from their possible inception from a stem cell is illustrated in Fig. 1. The major problem encountered in representing mathematically this proliferative scheme is in the mathematical representation of the proliferative compartments. One difficulty is the lack of precise knowledge of either the mean generation time or the mean transit time of cells in the proliferative compartments. Another difficulty is the lack of knowledge of the cell types of the daughters of a dividing cell. Perhaps the simplest and most appealing assumption in regard to the latter problem is the following scheme of proliferation: The stem cell is a self-maintaining compartment which produces myeloblasts. The myeloblast produces two promyelocytes when it divides. The promyelocyte in turn produces two myelocytes when it divides and the myelocyte, after one or two divisions in which the daughters are both myelocytes, divides again and produces two metamyelocytes [30].

However, the difficulty with the above model, or other simple models of proliferation that can be devised, is that mean generation times and other parameters can not be assigned to each of the proliferative compartments, which are consistent with the known observations regarding them, such as mitotic indices, DNA synthesis times, grain-count halving data, etc. The inconsistencies and inadequacies arising from one simple class of models, which includes the above-mentioned one, is discussed at length in the appendix. We conclude that it is premature, at the present time, to put forth a detailed model of the proliferative compartments which includes distinct stem, myeloblast, promyelocyte, and myelocyte compartments.

Until better quantified information regarding neutrophil precursors is forthcoming, we believe for modeling purposes, it is best to accept the view that there is a single self-maintaining proliferative pool [2, 23]. The cells in this pool can be

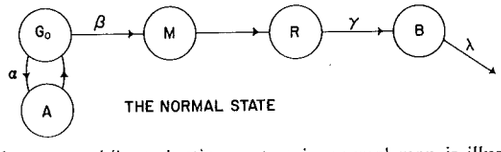

Fig. 9. The model of the neutrophil production system in normal man is illustrated schematically. The active compartment A and the resting compartment G_0 comprise the proliferative pool. The compartments labeled M, R, and B represent states of maturation, reserve, and circulating blood, respectively. The blood compartment includes the marginal granulocytes. The release rates α, β, and γ, which control the release of cells along the indicated pathways, depend on the total number of cells in the system (in the case of α and β) or in the blood (in the case of γ)

thought of as either representing myelocytes, the most common proliferative cell, or as representing the mean behavior, in some sense, of all the proliferative cells. As we will show, such a model is adequate to explain virtually all the known kinetic observations of cells in the blood (but not, of course, direct observations of the individual proliferative compartments).

The model we have introduced to represent neutrophil production system is illustrated in Fig. 9. The model consists of five pools or compartments. The proliferative pool is assumed to consist of two compartments, an active compartment A and a resting compartment G_0. The latter was originally introduced in order to show how the proliferative pool can respond dynamically to depletions in blood cells caused by unfavorable events, so as to renew itself rapidly [38]. The G_0 compartment fulfills the same function in our model. Thus, the specific nature of the granulopoietin story is not relevant to our model. The only biological assumption that is utilized in our model is that the control mechanism for cell production, whatever its complexities, is able to recognize the total number of neutrophils and their precursors.

By contrast, in the model of King-Smith and Morley [44], it is assumed that production is controlled by the number of mature neutrophils in the blood. We feel that it is more plausible to believe that, if the marrow was artificially depleted of granulocyte precursors, the production rate would immediately increase, rather than delay its response to this depletion until it reached the blood pool, many days later. In addition, because cells in G_0 leave at random, the time spent in the G_0 compartment is different for different cells. Furthermore, G_0 cells are acknowledged to be indistinguishable from G_1 cells, which are cells in the pre-synthetic phase of the fixed generation time interval characterizing the active compartment. Hence, the existence of the G_0 compartment also serves to make for a variable transit time of individual cells in the proliferating state, which is more in keeping with experience.

A cell which enters the active phase has a commitment to undergo cell division a fixed time T_A later. The generation time T_A is assumed to consist of four phases, G_1 the pre-synthetic phase, S the DNA synthetic phase, G_2 the post-synthetic phase, and M the mitotic phase. After mitosis, the two daughter cells produced by division enter the G_0 phase. In the G_0 phase, a certain portion of the cells leave at random to reenter the active compartment at a fractional rate α per unit time. Similarly, a certain portion of the cells leave at random to enter the maturation compartment at a fractional rate β per unit time.

The maturation compartment M is considered to be a "pipeline", in which all cells mature for a fixed time T_M and then enter the marrow reserve compartment R. The latter compartment is not a pipeline, but rather is, like G_0, a "random" compartment, because all cells are treated equivalently and can leave at random to enter the blood. The fractional rate at which cells leave the reserve compartment to enter the blood is γ. The reserve compartment contains the second control element in our model, namely, the ability of the marrow to release cells into the blood stream on demand. Here, too, we do not require any detailed nature of this leukocyte inducing or releasing factor. We assume only that the mechanism,

whatever its nature, is able to detect and respond to the number of neutrophils in the total blood granulocyte pool.

Because the interaction of cells in the blood with cells in the blood granulocyte reserve is largely unknown, and because the indications are that the rate of equilibration between these two pools is rapid, we have combined them into a single blood compartment. The latter is also a random compartment, from which cells disappear on die at random at a fractional rate per unit time λ.

To each compartment we assign a cell density function, which is assumed to be a function of either maturity and time, or age and time. The distinction is purely didactic, and we prefer to characterize the cell density functions for the pipeline compartments, namely the active compartment and the maturation compartment, as depending on maturity and time. In them, cells undergo maturation. The random compartments which comprise the G_0, reserve, and blood compartments, have associated with them cell density functions dependent on the age and time. In them, cells merely age without maturing, and they can in principle remain there a very long time. In distinction to the non-random compartments which have a fixed life-time associated with them, the random compartments have associated with them half-life times or mean lifetimes.

Let a represent age, μ represent maturity, and t represent time. The equations satisfied by the cell density functions are age-time equations of the form first suggested by Scherbaum and Rasch [68] and von Foerster [69], as follows.

$$\begin{aligned}
&\frac{\partial n(\mu,t)}{\partial t}+\frac{\partial n(\mu,t)}{\partial \mu}=0 && 0<\mu\leqq T_A,\\
&\frac{\partial g(a,t)}{\partial t}+\frac{\partial g(a,t)}{\partial a}=-(\alpha+\beta)\,g(a,t), && 0<a,\\
&\frac{\partial m(\mu,t)}{\partial t}+\frac{\partial m(\mu,t)}{\partial \mu}=0, && 0<\mu\leqq T_M, \qquad (1)\\
&\frac{\partial r(a,t)}{\partial t}+\frac{\partial r(a,t)}{\partial a}=-\gamma\, r(a,t), && 0<a,\\
&\frac{\partial b(a,t)}{\partial t}+\frac{\partial b(a,t)}{\partial a}=-\lambda\, b(a,t), && 0<a.
\end{aligned}$$

Here $n(\mu,t)$, $g(a,t)$, $m(\mu,t)$, $r(a,t)$, and $b(a,t)$ are the cell density functions in the active, G_0, maturation, reserve, and blood compartments, respectively. The age a or maturity μ characterizes each compartment separately, but the time t is the same variable in all compartments. For example, $a=0$ or $\mu=0$ always characterizes cells which are just entering a given compartment. The right hand side in these equations always represents cell loss. In order to represent leukopheresis experiments and other experiments in which external agents are introduced which cause cell loss or disappearance from a given compartment, a term $-D(\mu,t)$ (or $-D(a,t)$) must be added to the right hand side of a given compartment equation. Such a term represents the rate at which cells in the interval μ to $\mu+d\mu$ (or a to $a+da$) disappear at time t.

We assume that at any time t, the fractional loss rates α and β depend on the total population in all the compartments, $N(t)$. The specific functional dependence of α and β on $N(t)$ is taken to be as follows,

$$\alpha(t)=\alpha_0+\alpha_1\left[\left(\frac{\bar{N}}{N(t)}\right)^{\nu}-1\right], \tag{2}$$

$$\beta(t)=\alpha_0+\beta_1\left[\left(\frac{\bar{N}}{N(t)}\right)^{\nu}-1\right]. \tag{3}$$

Here α_0, α_1, β_1, $\bar{N}$, and ν are positive constants, and $\alpha_1>\beta_1$. The dependence of α and β on N is shown quantitatively in Fig. 10. We will show later that in the steady state of the system, $N=\bar{N}$, and $\alpha=\beta=\alpha_0$. The choice of the same exponent ν in equations (2) and (3) is made in the interest of simplicity, to reduce the number of free parameters appearing in the model. The functional dependence chosen permits the resting compartment to respond to depletions in the total population by increasing production, and by sending more cells to mature: $\alpha>\alpha_0$ and $\beta>\alpha_0$ when $N(t)<\bar{N}$. Contrariwise, if a state of overpopulation is for some reason achieved so that $N(t)>\bar{N}$, then less cells are produced or sent to maturity. The fact that $\alpha_1>\beta_1$ insures mathematically that the population is stable about the value $N=\bar{N}$, but we will not show this here.

The fractional loss rate in the blood λ is assumed to be a constant. The control of release of cells from the marrow reserve compartment to the blood is achieved in the model by permitting the reserve release rate γ to depend on the number of cells in the blood compartment $N_B(t)$, as follows,

$$\gamma=\gamma(t)=\begin{cases}\gamma_0+\gamma_1\left[\left(\dfrac{\bar{N}_B}{N_B(t-t_R)}\right)^{\rho}-1\right], & N_B(t-t_R)<\bar{N}_B,\\ \gamma_0, & N_B(t-t_R)\geqq\bar{N}_B.\end{cases} \tag{4}$$

Here γ_0, γ_1, $\bar{N}_B$, ρ and t_R are positive constants. The existence of a time delay t_R is indicated by various experiments, for example, the response to leukopheresis N_B represents the steady state value of the population in the blood compartment, so that in the steady state, $\gamma=\gamma_0$. According to equation (4), the release rate is increased whenever the blood population falls below its steady state value. However, if the blood is neutrophilic, then the marrow compartment releases cells at its minimum rate γ_0.

The cell density functions satisfy the following boundary conditions, which represent the manner in which new cells enter each compartment,

$$\begin{gathered}n(0,t)=\alpha N_0(t), \quad g(0,t)=2\,n(T_A,t), \quad m(0,t)=\beta N_0(t),\\ r(0,t)=m(T_M,t), \quad b(0,t)=\gamma N_R(t).\end{gathered} \tag{5}$$

Here $N_0(t)$ represents the total population in the resting compartment, and $N_R(t)$ represents the total population in the marrow reserve compartment. The factor 2 is present in the second equation in (5) to represent the fact that two cells are produced by division of the cells in the active compartment when they reach the age T_A.

In addition, the density functions satisfy an initial condition which specifies the initial state of the system,

$$\begin{gathered} n(\mu,0)=f_A(\mu), \quad g(a,0)=f_G(a), \quad m(\mu,0)=f_M(\mu), \\ r(a,0)=f_R(a), \quad b(a,0)=f_B(a), \end{gathered} \tag{6}$$

where the functions appearing on the right hand side above are all given.

The total compartment populations at any time are defined in terms of the cell density functions as follows,

$$\begin{gathered} N_A(t)=\int_0^{T_A} n(\mu,t)\,d\mu, \quad N_0(t)=\int_0^{\infty} g(a,t)\,da, \quad N_M(t)=\int_0^{T_M} m(\mu,t)\,d\mu, \\ N_R(t)=\int_0^{\infty} r(a,t)\,da, \quad N_B(t)=\int_0^{\infty} b(a,t)\,da. \end{gathered} \tag{7}$$

The total population $N(t)$ is defined as the sum of the compartment populations,

$$N(t)=N_A(t)+N_0(t)+N_M(t)+N_R(t)+N_B(t). \tag{8}$$

Because a time delay appears in the expression for γ, equation (4), we need to know $N_B(t-t_R)$ for $0\leqq t<t_R$. That information is given as follows,

$$N_B(t-t_R)=F_B(t), \qquad 0\leqq t<t_R, \tag{9}$$

where $F_B(t)$ is a prescribed function.

Equations (1) in conjunction with the boundary conditions (5) and the initial conditions (6) and (9) constitute the mathematical formulation of the model.

To represent experiments in which a label such as tritiated thymidine is introduced into those cells in the active compartment which are in S-phase, it is convenient to partition the active compartment into three compartments consisting of the G_1 cells, the S-phase cells, and the G_2+M cells. (If cells in mitosis need to be distinguished, the G_2+M cells can be subdivided further in the same manner.) Then the first equation appearing in (1) is replaced by the three equations

$$\begin{aligned} &\frac{\partial n_1(\mu,t)}{\partial t}+\frac{\partial n_1(\mu,t)}{\partial \mu}=0, \qquad 0<\mu\leqq T_1, \\ &\frac{\partial n_s(\mu,t)}{\partial t}+\frac{\partial n_s(\mu,t)}{\partial \mu}=0, \qquad 0<\mu\leqq T_s, \\ &\frac{\partial n_2(\mu,t)}{\partial t}+\frac{\partial n_2(\mu,t)}{\partial \mu}=0, \qquad 0<\mu\leqq T_2, \end{aligned} \tag{10}$$

Here $n_1(\mu,t)$, $n_s(\mu,t)$, and $n_2(\mu,t)$ are the cell density functions for the G_1, S, and G_2+M phases, and T_1, T_s, and T_2 are the respective transit times of cells in these phases, where

$$T_1+T_s+T_2=T_A. \tag{11}$$

The first two boundary conditions in (5) are replaced by the set of boundary conditions,

$$n_1(0,t)=\alpha N_0(t), \qquad n_s(0,t)=n_1(T_1,t),$$
$$n_2(0,t)=n_s(T_s,t), \qquad g(0,t)=2n_2(T_2,t). \tag{12}$$

In addition, the first initial condition in (6) is replaced by the set of initial conditions

$$n_1(\mu,0)=f_1(\mu), \qquad n_s(\mu,0)=f_s(\mu), \qquad n_2(\mu,0)=f_2(\mu), \tag{13}$$

where f_1, f_s, and f_2 are prescribed functions of μ. The populations N_1, N_s, and N_2 of the subcompartments G_1, S, and G_2+M of the active compartment, respectively, are defined as

$$N_1(t)=\int_0^{T_1} n_1(\mu,t)\,d\mu, \qquad N_s(t)=\int_0^{T_s} n_s(\mu,t)\,d\mu, \qquad N_2(t)=\int_0^{T_2} n_2(\mu,t)\,d\mu. \tag{14}$$

4. The Steady State Behavior of the System

It is possible to obtain the solution to the model equations when the system is in a steady state. Then the initial conditions (6) and the time derivatives appearing in equations (1) are disregarded, and the following steady state solutions, denoted by an overbar, can be found readily,

$$\begin{aligned} &\bar{n}(\mu)=n_0, && 0\leqq\mu\leqq T_A,\\ &\bar{g}(a)=g_0\,e^{-2\alpha_0 a}, && 0\leqq a,\\ &\bar{m}(\mu)=m_0, && 0\leqq\mu\leqq T_M,\\ &\bar{r}(a)=r_0\,e^{-\gamma_0 a}, \quad \bar{b}(a)=b_0\,e^{-\lambda a}, && 0\leqq a, \end{aligned} \tag{15}$$

where n_0, g_0, m_0, r_0, and b_0 are constants. The solutions for g, r, and b depended on the provisional assumption that N_B and N were equal to $\bar{N}_B$ and $\bar{N}$, respectively. We find in fact by substituting (15) into (7) and integrating, that the compartment populations are constant, and we denote the constant steady state values so derived with an overbar. Thus,

$$\begin{gathered} \bar{N}_A=n_0\,T_A, \qquad \bar{N}_0=g_0/2\,\alpha_0, \qquad \bar{N}_M=m_0\,T_M,\\ \bar{N}_R=r_0/\gamma_0, \qquad \bar{N}_B=b_0/\lambda. \end{gathered} \tag{16}$$

Hence, the total population $N(t)$ is also a constant denoted by $\bar{N}$, and given by the expression

$$\bar{N}=\bar{N}_A+\bar{N}_0+\bar{N}_M+\bar{N}_R+\bar{N}_B. \tag{17}$$

The solution (15) must satisfy the boundary conditions (5). Note that in the latter equations, the fractional loss rates α, β, and γ assume the constant values, according to equations (2)—(4),

$$\alpha=\alpha_0, \qquad \beta=\alpha_0, \qquad \gamma=\gamma_0. \tag{18}$$

The result is

$$g_0=2n_0, \qquad m_0=g_0/2=n_0, \qquad r_0=g_0/2=n_0, \qquad b_0=r_0=n_0. \tag{19}$$

If we substitute this set of equations into (16), we find that the compartment populations can all be expressed in terms of the single constant n_0, which represents the steady state production rate of the system:

$$\bar{N}_A = n_0\, T_A, \qquad \bar{N}_0 = n_0/\alpha_0, \qquad \bar{N}_M = n_0\, T_M,$$
$$\bar{N}_R = n_0/\gamma_0, \qquad \bar{N}_B = n_0/\lambda. \tag{20}$$

The last equation above expresses the fact that the steady state production rate n_0 equals the steady state loss from the blood compartment $\lambda\, \bar{N}_B$. From (17) and (20) total population can also be expressed in terms of n_0 as

$$\bar{N} = n_0\,(T_A + \alpha_0^{-1} + T_M + \gamma_0^{-1} + \lambda^{-1}). \tag{21}$$

From equation (21) and the last of equations (20) (any one of them will do) we can eliminate n_0 and so deduce the following compatibility condition which the parameters of the system must satisfy,

$$\bar{N} = \bar{N}_B\, \lambda\,(T_A + \alpha_0^{-1} + T_M + \gamma_0^{-1} + \lambda^{-1}). \tag{22}$$

If the subcompartments of N_A are introduced and equations (10) replace the first of equations (1), then the steady state solutions for it are as follows,

$$n_1 = n_s = n_2 = n_0, \qquad \bar{N}_1 = n_0\, T_1,$$
$$\bar{N}_s = n_0\, T_s, \qquad \bar{N}_2 = n_0\, T_2. \tag{23}$$

Of course, $\bar{N}_A = \bar{N}_1 + \bar{N}_s + \bar{N}_2$.

5. Integration of the Kinetic Equations

Because of the assumed dependence of α, β, and γ on $N(t)$ and $N_B(t)$, the equation system (1) is nonlinear, and so we can not expect to obtain an analytical solution of it. However, it is possible to derive the equations that the total compartmental populations $N_A(t)$, $N_0(t)$, etc. must satisfy, by integration of equations (1) over age or maturity, as needed. We illustrate this procedure in detail for the active compartment.

Integrating the first equation in (1) over μ, and utilizing (7), we find that

$$\frac{d\,N_A(t)}{d\,t} + n\,(T_A, t) - n\,(0, t) = 0. \tag{24}$$

The general solution of the cell density equation without regard to the initial condition or the boundary condition is an arbitrary function of $t-\mu$. Therefore,

$$n\,(\mu, t) = n\,(\mu - t, 0), \qquad t \leqq \mu,$$
$$n\,(\mu, t) = n\,(0, t-\mu), \qquad t > \mu. \tag{25}$$

For $t < \mu$, in view of the initial condition (6),

$$n\,(\mu, t) = f_A\,(\mu - t), \qquad t \leqq \mu. \tag{26}$$

Hence, the function $n\,(T_A, t)$ appearing in (24) is given by the expression

$$n(T_A, t)=\begin{cases} f_A(T_A-t), & t\leqq T_A, \\ n(0, t-T_A), & t>T_A. \end{cases} \tag{27}$$

Substituting (27) and the boundary condition (5) into (24) leads to the following difference-differential equation that $N_A(t)$ must satisfy,

$$\frac{dN_A}{dt}=\alpha(t)N_0(t)-\begin{cases} f_A(T_A-t), & 0<t\leqq T_A, \\ \alpha(t-T_A)N_0(t-T_A), & t>T_A. \end{cases} \tag{28}$$

In a similar manner, we readily derive the following equations that the other compartmental populations satisfy,

$$\begin{aligned} \frac{dN_0}{dt}&=-[\alpha(t)+\beta(t)]N_0(t)+2\begin{cases} f_A(T_A-t), & 0<t\leqq T_A, \\ \alpha(t-T_A)N_0(t-T_A), & t>T_A, \end{cases} \\ \frac{dN_M}{dt}&=\beta(t)N_0(t)-\begin{cases} f_M(T_M-t), & 0<t\leqq t_M, \\ \beta(t-T_M)N_0(t-t_M), & t>T_M, \end{cases} \\ \frac{dN_R}{dt}&=-\gamma(t)N_R(t)+\begin{cases} f_M(T_M-t), & 0<t\leqq T_M, \\ \beta(t-T_M)N_0(t-T_M), & t>T_M, \end{cases} \\ \frac{dN_B}{dt}&=-\lambda N_B(t)+\gamma(t)N_R(t), \end{aligned} \tag{29}$$

where $\gamma(t)$ is given by (4) for $t\geqq t_R$ and by the expression

$$\gamma(t)=\begin{cases} \gamma_0+\gamma_1\left[\left(\dfrac{\bar{N}_B}{F_B(t)}\right)^{\nu}-1\right], & F_B(t)<\bar{N}_B, \\ \gamma_0, & F_B(t)\geqq\bar{N}_B, \end{cases} \tag{30}$$

for $0\leqq t<t_R$.

When three subcompartments replace the active compartment as in (10), equation (28) and the first equation in (29) gets replaced by the following three equations, obtained by integrating (10) over the maturation and/or age variables,

$$\begin{aligned} \frac{dN_1}{dt}&=\alpha(t)N_0(t)-J_1, \\ \frac{dN_s}{dt}&=J_1-J_s, \\ \frac{dN_2}{dt}&=J_s-J_2, \\ \frac{dN_0}{dt}&=2J_2-[\alpha(t)+\beta(t)]N_0(t), \end{aligned} \tag{31}$$

where

$$J_1=\begin{cases} f_1(T_1-t), & 0<t\leqq T_1, \\ \alpha(t-T_1)N_0(t-T_1), & t>T_1, \end{cases}$$

$$J_s=\begin{cases} f_s(T_s-t), & 0<t\leqq T_s, \\ f_1(T_1+T_s-t), & T_s<t\leqq T_1+T_s, \\ \alpha(t-T_1-T_s)N_0(t-T_1-T_s), & t>T_1+T_s, \end{cases} \tag{32}$$

$$J_2 = \begin{cases} f_2(T_2 - t), & 0 < t \leqq T_2, \\ f_s(T_s + T_2 - t), & T_2 < t \leqq T_2 + T_s, \\ f_1(T_A - t), & T_2 + T_s < t \leqq T_A, \\ \alpha(t - T_A) N_0(t - T_A), & t > T_A. \end{cases}$$

In (31), the right hand side is always the difference between cell influx and cell outflux. The factor 2 in the last equation in (31) accounts for cell division that takes place when cells leave compartment 2.

The set of equations (28) and (29) can be readily integrated numerically with the aid of a computer. This integration requires the initial values of the compartment populations $N_A(0)$, $N_0(0)$, $N_M(0)$, $N_R(0)$, $N_B(0)$, the function $F_B(t)$ appearing in (9), and the initial maturity distribution functions $f_A(\mu)$, and $f_M(\mu)$. When equations (31) are to be utilized, the initial maturity distribution $f_A(\mu)$ must be partitioned into $f_1(\mu)$, $f_s(\mu)$, and $f_2(\mu)$. This partitioning also implies the values of $N_1(0)$, $N_s(0)$, and $N_2(0)$, which are needed. Furthermore, the values of the 13 parameters T_A, T_M, t_R, α_0, α_1, β_1, γ_0, γ_1, λ, $\bar{N}$, $\bar{N}_B$, ν and ρ must be specified, subject to the equation of constraint (22). When the equation system is enlarged so that G_1, S, and $G_2 + M$ compartments replace the active compartment, we must specify in place of T_A the compartmental transit times T_1, T_s, and T_2, respectively.

6. Determinations of the Values of the Parameters

One of the principal purposes in constructing our model was to determine whether the known facts of neutrophil production and control could be organized and understood within the framework of a single comprehensive quantitative mathematical model. As we have just seen, the model contains 13, or in its augmented form, 15 disposable parameters. Nevertheless, there is a large body of information with which the system must be shown to be consistent. We indicate here how the parameter determination was made.

We shall assume that the observations reported in section 1, unless otherwise noted, are representative of the steady state behavior of the neutrophil production system of a normal 70 kgm man. Therefore the following quantitative inferences are more or less fixed by observation.

In the steady state:

1. Labeling index (L.I.) of marrow proliferative cells $= 0.3$.
2. Mean transit time in marrow proliferative pool $= 50$ hr.
3. Synthesis time of proliferative cells $T_s = 15$ hr.
4. Earliest time for entry of labeled synthesis cells into maturation compartment $= 3$ hr $= T_2$.
5. Obligatory transit time of nonproliferating marrow cells $= 4$ days $= T_M$.
6. Half-life of blood cells $T_{1/2} = 6.7$ hr or $\lambda = 0.103$/hr.

7. Total number of cells in the circulating blood plus marginal granulocyte pool is $N_B = 4.9 \cdot 10^{10}$ cells/70 kgm man.
8. Ratio of nonproliferating to proliferating cells in the marrow = 3.72.

From these observations, we see that the parameters T_s, T_2, T_M, λ, and $\bar{N}_B$ are relatively unambiguously determined. The theoretical values of some of the other observed quantities are as follows. The labeling index is the fraction of all proliferative cells which take up tritiated thymidine. Assuming all cells in S-phase and no other cells become labeled, then the labeling index in the steady state is given as

$$\text{L. I.} = \frac{\bar{N}_s}{\bar{N}_A + \bar{N}_0} = \frac{T_s}{T_A + 1/\alpha_0}. \tag{33}$$

Here, we have introduced the steady state values of the compartment populations from equations (20) and (23).

The mean age of a cell in the G_0 compartment in the steady state is given with the aid of equation (15) as

$$\frac{1}{N_0} \int_0^\infty a\, g_0\, e^{-2\alpha_0 a}\, da = \frac{1}{2\alpha_0}. \tag{34}$$

This mean age is also the mean age at which a cell leaves the G_0 compartment, or the mean transit time of a cell entering G_0.

The mean lifetime of a cell in the proliferative pool in the steady state can be defined as the mean time that a cell persists through many divisions in the proliferative pool. For this purpose, one of the daughters resulting from a cell division must be identified as the original cell. Thus, a cell that has just entered the G_0 compartment persists in it for a mean time $1/(2\,\alpha_0)$. Then, with probability 1/2, it goes through the active compartment for a period T_A and again persists in the G_0 compartment for a mean time $1/(2\,\alpha_0)$. Therefore, the contribution of this sojourn to its lifetime in proliferation is $\frac{1}{2}[T_A + 1/(2\,\alpha_0)]$. Then, with probability 1/2, it repeats this cycle, contributing $(\frac{1}{2})\,[T_A + 1/2\,\alpha_0]$ to its mean lifetime. By summation, the total mean lifetime in proliferation is given as

$$\text{Mean lifetime in proliferation} = \frac{1}{2\,\alpha_0} + \sum_{n=1}^{\infty} \left(\frac{1}{2}\right)^n \left[T_A + \frac{1}{2\,\alpha_0}\right] = T_A + \frac{1}{\alpha_0}. \tag{35}$$

An alternative concept that has been introduced is the mean cell transit time, defined as the total population divided by the production rate. According to this definition,

$$\text{Mean cell transit time in proliferation} = \frac{\bar{N}_A + \bar{N}_0}{n_0} = T_A + \frac{1}{\alpha_0}, \tag{36}$$

with the aid of (20). Hence, the mean life time and the cell transit time are equal, in the present model.

A related quantity of interest is the interdivision time, defined as the mean time that a cell spends in the proliferative pool between its birth and the time it

divides. This time is the sum of the mean times it spends in G_0 and the active compartment, respectively, or,

$$\text{Mean interdivision time} = T_A + \frac{1}{2\,\alpha_0}. \tag{37}$$

It is by no means a trivial matter to decide which of the above defined times a given experiment is measuring, if any. The observations numbered 1.—3. above are all consistent with a mean life time in the proliferative pool of 50 hrs. This is so whether mean generation time is interpreted as mean cell transit time as in equation (35) and inferred from relative marrow populations in the proliferative pool and mitotic indices [5, 20], or from the half-life of radioactively labeled proliferative cells as inferred from the decay time of their average grain count [19]. This decay time may be expected to equal approximately the mean cell transit time.

In principle, the interdivision times could be determined from the labeled mitosis curves. If we knew both the interdivision time and the mean generation time, we could infer the values of both T_A and α_0 uniquely. Unfortunately, the few available observations [17] are not sufficiently quantified to permit an unambiguous interpretation in this regard. Furthermore, the interpretation is obscured by the fact that three types of proliferative cells, myeloblasts, promyelocytes, and myelocytes, are represented in the labeled mitosis curves. Consequently, it is difficult to determine the relative contributions of T_A and $1/\alpha_0$ to their sum. The only direct determination of the interdivision time of myelocytes was made in vitro [21], and found to be 30 hrs. At first sight, it would appear that we should set the theoretical interdivision time $T_A + \frac{1}{2\,\alpha_0} = 30$ hr. This implies that $1/\alpha_0 = 40$ hr, and $T_A = 10$ hr. However, the minimum value of T_A possible is 18 hr, based on the values $T_s = 15$ hr, $T_2 = 3$ hr (see observation 4 above), and an assumed minimum value $T_1 = 0$ for cells in G_1 phase. Therefore, it appears more plausible to assume that this observation represents a determination of the minimum possible cell transit time, or T_A. Based on this interpretation and the inferred value of $T_A + \frac{1}{\alpha_0} = 50$ hr, we infer that $1/\alpha_0 = 20$ hr, and $\alpha_0 = 0.05$/hr. It should be noted that the maximum value T_A could approach is 50 hr. However, this would be at the expense of making α_0 very large. The latter in turn would make the population in G_0 very small, and would probably seriously compromize the ability of the system to maintain homeostatic control of the total population.

The ratio of nonproliferating to proliferating marrow cells in the steady state is, with the aid of equations (20), given by the expression

$$\frac{\text{Non-proliferating marrow cells}}{\text{Proliferating marrow cells}} = \frac{\bar{N}_M + \bar{N}_R}{\bar{N}_A + \bar{N}_0} = \frac{T_M + 1/\gamma_0}{T_A + 1/\alpha_0}. \tag{38}$$

When this ratio is set equal to 3.72, and combined with $T_A + 1/\alpha_0 = 50$ hr and $T_M = 96$ hr, we find that $1/\gamma_0 = 90$ hr. For some calculations this value was increased to $1/\gamma_0 = 96$ hr, so that $1/\gamma_0 = T_M$. A longer marrow transit time is suggested by the BGSA curve reported in Fig. 3. Choosing $1/\gamma_0 = 96$ hr makes the populations

in the reserve compartment and the maturation compartment exactly equal, and suggests, on the basis of the relative population of the marrow cell types, that all the segmented granulocytes plus a small portion of the band cells constitute the marrow reserve compartment.

From the known values of $\bar{N}_B$, T_A+1/α_0, T_M, $1/\gamma_0$, and λ, the total neutrophil population is deduced from the steady state compatibility relation (22) to be $\bar{N}=1.24\cdot 10^{12}$ cells, which is not too different from the observed number [26]. Thus, the steady state parameters of the system, namely, $\bar{N}_B$, $\bar{N}$, T_A, $1/\alpha_0$, T_M, $1/\gamma_0$, and λ are all determined in a more or less consistent and unambiguous manner from experiment, with the possible exception of the values of T_A and $1/\alpha_0$.

To summarize, the production rate, transit times, and populations in the various compartments in the steady state are inferred or deduced to be as shown in Table 4.

Table 4. *Values of the Steady State Parameters*

Inferred from Experiments	Deduced
$T_2=3$ hr,	$n_0=5.0\cdot 10^9$ cells/hr,
$T_s=15$ hr,	
$T_A=30$ hr,	$\bar{N}_A=1.51\cdot 10^{11}$ cells,
$1/\alpha_0=20$ hr,	$\bar{N}_0=1.01\cdot 10^{11}$ cells,
$T_M=96$ hr,	$\bar{N}_M=4.85\cdot 10^{11}$ cells,
$1/\gamma_0=90$ hr,	$\bar{N}_R=4.54\cdot 10^{11}$ cells,
$1/\lambda=9.7$ hr,	$\bar{N}=1.24\cdot 10^{12}$ cells,
$\bar{N}_B=0.49\cdot 10^{11}$ cells,	Total transit time=246 hr

The deduced production rate n_0 is equivalent to a production rate of $1.68\cdot 10^9$ cells (kgm/day).

There still remains the problem of determining what may be called the dynamic parameters of systems, α_1, β_1, γ_1, ν, ρ, and t_R. These parameters enter into the homoestatic control elements α, β, and γ. Hence, these values can be inferred only from experiments which perturb the steady state behavior of the system. The observations of such behavior are qualitative or at best semi-quantitative. Therefore, we resorted to numerical solution of the governing differential equations, for various choices of these parameters, and relied on qualitative agreement with the known observations to determine their values.

In order to simplify this determination, we made the following arbitrary assumptions,

$$\alpha_1=\alpha_0, \qquad \beta_1=\tfrac{1}{2}\alpha_0, \qquad \gamma_1=\gamma_0, \qquad \rho=\nu. \tag{39}$$

Note that stability of the system requires that $\beta_1<\alpha_1$ and that α_0 is a fairly small quantity. In the absence of any information regarding it, $\beta_1=\frac{1}{2}\alpha_1$ seemed to be a plausible first guess. The assumption that $\rho=\nu$ implies that the dynamical response to LIF which controls the maintenance of the normal blood neutrophil

population at the level $\bar{N}_B$ is the same as the dynamical response of the system to granulopoietin which maintains the total neutrophil populations at the normal level $\bar{N}$. There is no biological reason for making this assumption. By making it, however, we are left with only two dynamical parameters to determine, t_R and v.

7. Results and Discussion

The theoretical blood-granulocyte-specific-activity curve was calculated by solving equations (29) and (31) numerically. We assumed that at $t=0$, the cells were in a steady state, and that all cells in S-phase were labeled with a label value of 1,

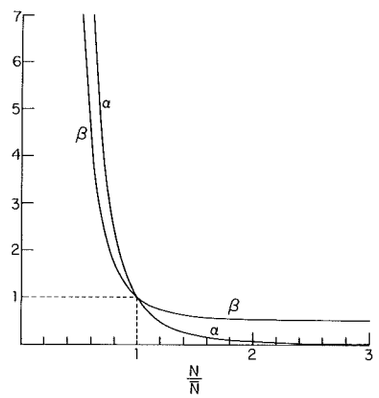

Fig. 10. The release rates α and β are shown as a function of $N(t)/\bar{N}$, according to equations (2) and (3), with $v=4$ and $\alpha_1/\alpha_0=2$ $\beta_1/\alpha_0=1$. The ordinate unit is α_0

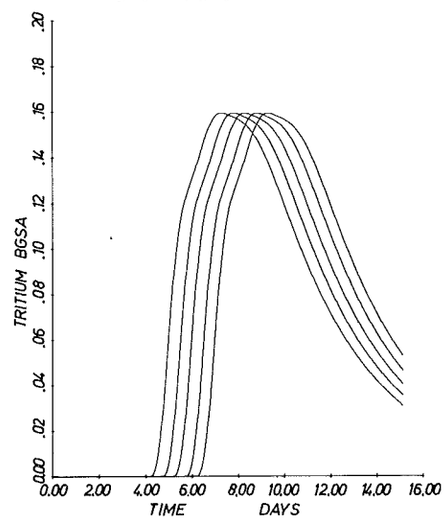

Fig. 11. The theoretical tritium blood-granulocyte-specific-activity (BGSA) curves are shown for five different assumed values of the obligatory transit time of nonproliferative marrow cells, $T_M=96$, 108, 120, 132, and 148 hr. Successively larger values of T_M correspond to the successively later onsets of appearance of labeled cells. Other parameter values are as shown in Table 4. Compare the experimentally observed curves shown in Fig. 2

an arbitrary unit of activity. Following division, it was assumed that a cell contributes half of its label value to each of its daughters. All cells with a label value of 1/4 or more were followed. The resulting value of the label value or activity of blood cells, called the tritium BGSA, was determined as a function of the time, by summing the total number of labeled cells in the blood compartment, multiplied by their appropriate label value. The result is shown in Fig. 11 for several assumed values of T_M. The curve for $T_M=96$ hr is in qualitative agreement with the experimental curve shown in Fig. 2. The fact that the theoretical curve begins approximately four days after the initial labeling time is in quantitative agreement with experiment. Of course, this anticipated agreement formed the basis of the selection of the value of T_M. In the same manner, a theoretical BGSA curve following exposure to DFP^{32} label was calculated numerically from equations (28) and (29). It was assumed that at $t=0$, the population was in a steady state and that all cells in the blood, proliferating compartments (G_0 and active), and nonproliferating compartments (maturation and reserve), were labeled with label values 4, 2, and 1, respectively.

The resulting computer generated curves are shown in Fig. 12, for three assumed values of the mean transit time in the maturation compartment, $T_M=4$, 5, and 6 days, and $1/\gamma_0=96$ hr. These values correspond to a total transit time in the marrow nonproliferating pool of 8, 9, and 10 days, respectively. The ordinate represents the activity of cells in the blood, normalized to its initial value, in arbitrary units. The curves display a good qualitative agreement with the experimental results of Fig. 3. There is a "bump" in the theoretical curve following the

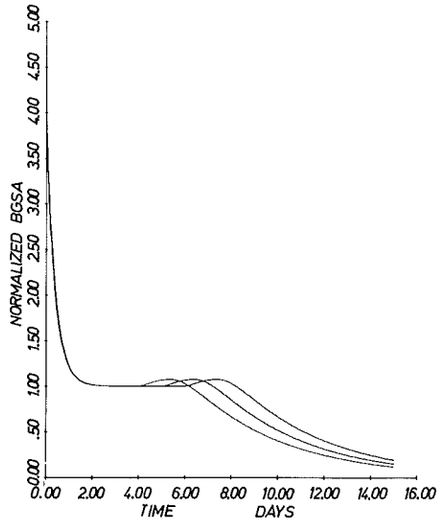

Fig. 12. The theoretical BGSA curve following DFP^{32} labeling is shown for the three different values $T_M=96$, 120, and 148 hr. The more extended curves correspond to the larger values of T_M, in sequence. Other parameter values are as shown in Table 4 with the exception that $1/\gamma_0=96$ hr. Compare the experimental points shown in Fig. 3

horizontal portion of the curve, which is present because of the appearance of some proliferative cells from the G_0 compartment with label value 2. Such a bump is perhaps also present in the curve shown in Fig. 3. The theoretical curves of Fig. 11 and others that we calculated, show that the horizontal portion of the curve is extended by increasing the assumed value of T_M, but not extended particularly by increasing $1/\gamma_0$. The experimental curves do have a horizontal portion of the curve that is more extended than that produced by the model. However, the value of T_M can not be altered greatly without disturbing the agreement of the theory with the experimental curves of Fig. 2. We conclude from this comparison that the reserve compartment is more complicated than we have assumed, i.e., it appears to possess both "pipeline" and "random" characteristics. It probably behaves more like a "pipeline" compartment in steady state, and exhibits more of its "random" releasing properties in response to demand.

The mean transit time of cells through the system, which we inferred to be 10 1/4 days, tends to agree with the larger estimate of 11.4 days inferred from Fig. 3 [6], than with the other shorter estimates which were cited [24, 25]. In fact, a comparison of the theoretical curves shown in Figs. 11 and 12 corresponding to $T_M=96$ hr (curves on the extreme left) indicate that the peak in the tritium BGSA curve (Fig. 11) should appear at approximately the same place that BGSA curve (Fig. 12) begins to fall below unity. Although such coincidence is observed in the dog [2], it is not observed in humans, as Figs. 2 and 3 show. This lack of coincidence has already been noted, with the suggestion that DFP^{32} data is more representative of normal transit times [2].

To simulate the effect of leukopheretic studies, a death term $-D(t)\,b(a,t)$ was added to the last equation appearing in equations (1). The function $D(t)$ was assumed to be

$$D(t)=f_0 \sum_{j=1}^{K} \delta\left(t-(j-1)\,t_0\right), \tag{40}$$

where δ is the Dirac delta function, f_0 and t_0 are constants, and K is an integer. This term represents the removal of a fraction of cells f_0 per unit time from the blood population at equal intervals t_0 starting at $t=0$, and ending, after K removals, at time $t=(K-1)\,t_0$. The introduction of this term leads to the appearance of a loss term $-D(t)\,N_B(t)$ on the right hand side of the last equation in (29). Equations (28) and (29) were then integrated numerically, as before.

The value of $t_R=3$ hr was chosen to represent the rapid recovery seen in leukopheretic experiments [27–29]. Figs. 13 and 14 show the theoretical response of the normalized blood cell population $N_B(t)/\bar{N}_B$ to a single leukopheresis at $t=0$. In Fig. 13, f_0 was chosen to be 0.25, representing a removal of 25% of the total population in the blood compartment at $t=0$, and $v=3, 4$. Fig. 13 a shows the short term population response during the first 3 days, and Fig. 13 b shows the long term response over a period of 200 days. For Fig. 14, the curves were repeated with $f_0=0.50$ representing a removal of 50% of the total blood population at $t=0$. The initial peak of recovery of the cell population observed in the blood was found to depend sensitively on the choice of v. Larger values of v intensify the response and produce larger peak or overshoot values, as expected.

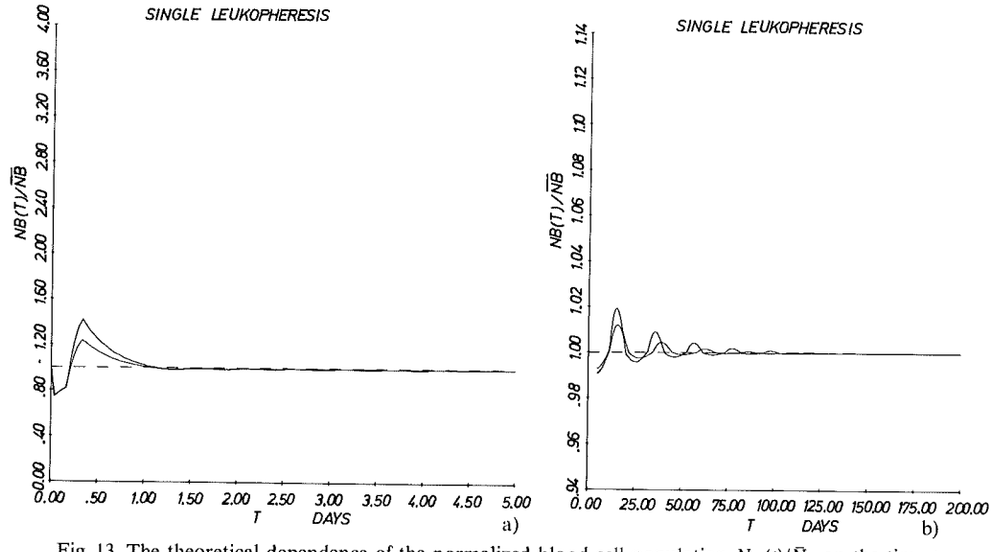

Fig. 13. The theoretical dependence of the normalized blood cell population $N_B(t)/\bar{N}_B$ on the time t following a single leukopheresis of 25% of the blood neutrophils at $t=0$. The blood cells were previously assumed to be in a steady state. The dashed line represents the normal steady state blood level. The curve with the larger initial peak corresponds to $\nu=4$, and the curve with the smaller peak correspond to $\nu=3$. Other parameter values are as shown in Table 4 and equation (39), and $t_R=0.3$ hr. In a), the response is shown for the first 5 days, and in b), the response is shown from $t=5$ days to $t=200$ days

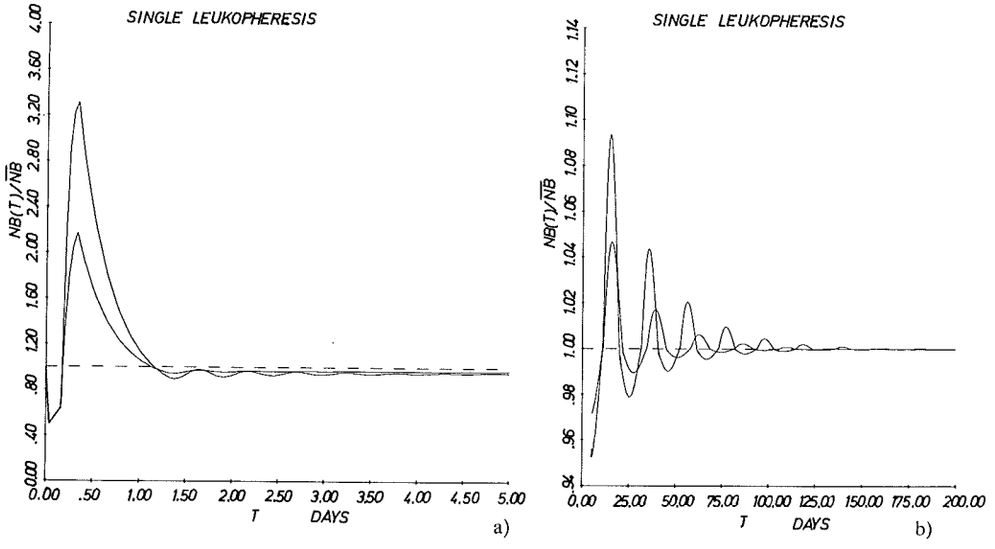

Fig. 14. The theoretical dependence of the normalized blood cell population $N_B(t)/\bar{N}_B$ on the time t following a single leukopheresis of 50% of the blood neutrophils at $t=0$. Other parameters and details are as for Fig. 13

Also, as can be seen by comparing Figs. 13 a and 14 a, a larger value of the leukopheretic parameter f_0 produced a larger overshoot response. This overshoot response is a feature that is to be expected of the nonlinear control feature of the model represented by the function $\gamma(t)$.

A characteristic of the predicted response of the system is the cyclic variation or "ringing" of the blood cell population, which persists for a fairly long time. However, it is seen in Figs. 13 b and 14 b that these oscillations have a small amplitude compared to the unperturbed level.

This oscillation is presumably due to the presence of the total neutrophil population control element, as represented by $\alpha(t)$ and $\beta(t)$. No such oscillations of either type have been reported in leukopheretic experiments, although neither has the quantitative dependence of the cell population as a function of the time been reported. One quantitative report of the initial response only of the blood cell population of the dog in response to acute infection [31] does show an initial oscillatory behavior, of rather large amplitude, with a period of about two days (see Fig. 4).

It seems important to determine whether such oscillations do in fact occur, and what their quantitative behavior is, because such behavior has an important bearing on the nature of the regulatory mechanism controlling the blood neutrophil population. Our calculations, based on large perturbations of the system, suggest that such oscillation should be very difficult to observe. It is important to bear in mind that actual observations may reflect a dynamic exchange of cells between the circulating blood cells and the marginal granulocyte pool. The model does not permit any such exchange, and we are aware of this shortcoming of the model. The simplification of our model in this manner was dictated by the absence of any quantitative experimental information to guide us in suitably constructing a more complicated model.

As previously mentioned, long term cyclic variations of the neutrophil blood population have been occasionally observed in normal subjects [42, 43], as illustrated in Fig. 8. They are also a feature of the disease state cyclic neutropenia. Our calculations suggest that such observations are manifestations of disturbances in the control elements of the neutrophil production system.

Our model has some features in common with the computer model of King-Smith and Morley [44], which contains control elements regulating the rate of release of marrow reserve cells to the blood, and the rate of production of new cells. The principal purpose of their model, however, was not to simulate the entire production scheme of neutrophils, but to show how a feed back control system simulated, in a qualitative manner, the periodicities believed to have been seen in granulopoiesis.

There are some significant differences between the model of King-Smith and Morley and the present model which should be remarked upon, even though a complete description of the model of these authors has not been reported yet. In their model, the production rate apparently depends on the blood neutrophil concentration, while in our model it is governed by the total population of the

neutrophils. It seemed more plausible to us that if, say, marrow cells alone were destroyed at a given time, the system would immediately start to replenish itself without waiting for a deficit to appear in the blood. Such a response is perhaps suggested by the recovery of blood neutrophils of the dog seen in response to

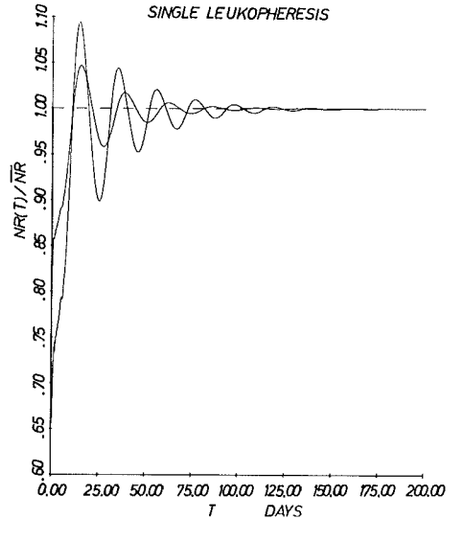

Fig. 15. The theoretical dependence of the normalized marrow reserve population $N_R(t)/\bar{N}_R$ on the time t for the same case as in Fig. 14

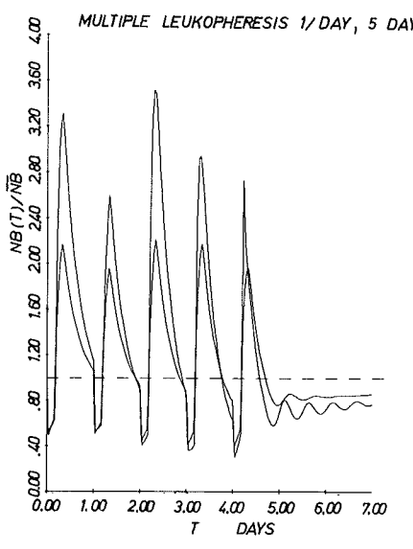

Fig. 16. The theoretical dependence of the normalized blood cell population $N_B(t)/\bar{N}_B$ as a function of the time t, in response to multiple leukopheresis of 50% of the blood neutrophils over a period of 1 hr, and carried out every day for five days, beginning at $t=0$. The parameter values are as in Table 4 and equations (39), with $t_R=3$ hr and $v=4$

marrow depressing drugs [30]. King-Smith and Morley found that a stable small aplitude oscillation was established in response to marrow failure. We find that although the long term oscillation is present, it is of small amplitude and damps out slowly. This finding suggests a possible reason why cyclic oscillations of the neutrophil count is only rarely (if ever) observed in healthy individuals — it is only detectable when the neutrophil production system has been strongly perturbed in some manner, and the time of perturbation is sufficiently recent to the time of observation.

Fig. 15 displays the behavior of the normalized marrow reserve population $N_R(t)/\bar{N}_R$ in response to a single leukopheresis of 50% of the blood cells. It is seen that the small amplitude oscillatory behavior of the blood population is common to this population too. Fig. 16 shows the result of multiple leukopheresis of the normalized blood population $N_B(t)/\bar{N}_B$, amounting to 50% of the blood neutrophils, and carried out once a day for five days. The figure shows that an immediate overshoot phenomenon occurs in response to each leukopheresis.

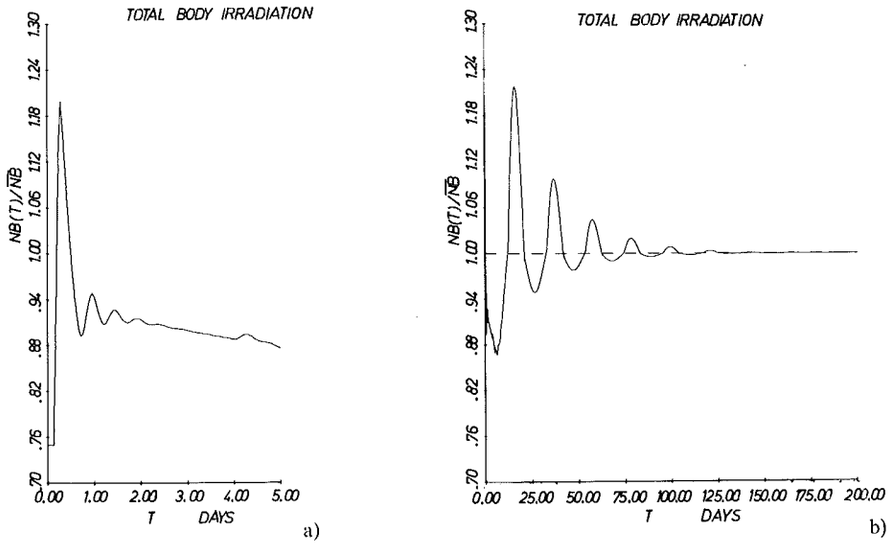

Fig. 17. The theoretical dependence of the normalized blood population $N_B(t)/\bar{N}_B$ on the time t, in response to a total body irradiation which eliminates 25% of the total neutrophil population, uniformly in each compartment. The behavior for the first 5 days is shown in a), and for 200 days in b). The parameter values are the same as for Fig. 16. A temporary neutrophilia develops in the blood in spite of the large initial depletion of the total neutrophil population

Total body irradiation experiments were simulated by assuming that a steady state population was suddenly decreased by a fixed fraction in all compartments at $t=0$. Fig. 17 shows the response of the normalized blood population to a depletion of 25% of the population in each compartment. In Figs. 17 a and 17 b the near term and long term behavior, respectively, is displayed. These results are very similar to the response of the system to a single leukopheresis. The long term oscillatory behavior of the blood population and its gradual decay is

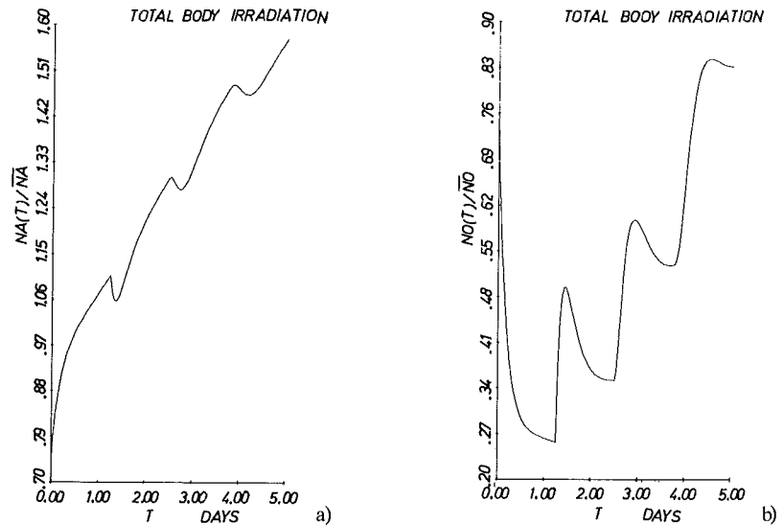

Fig. 18. The theoretical response of the normalized populations a) $N_A(t)/\bar{N}_A$, b) $N_0(t)/\bar{N}_0$, c) $N_M(t)/\bar{N}_M$, and d) $N_R(t)/\bar{N}_R$, in the active, resting, maturation, and reserve compartments, respectively, as a function of the time, following a total body elimination of 25% of the population, uniformly in each compartment, at $t=0$. Parameter values are as for Fig. 16. The response is shown for the first five days

already in evidence. Perhaps the most notable difference between the two cases is that the amplitude of the oscillation and the initial amount of overshoot is somewhat larger in the case of total body irradiation, when the total cell loss is much larger.

Figs. 18 a—18 d display the near term response of the marrow proliferative and nonproliferative populations $N_A(t)/\bar{N}_A$, $N_0(t)/\bar{N}_0$, $N_M(t)/\bar{N}_M$, and $N_R(t)\bar{N}_R$, respectively, for a period of 5 days. We see in Fig. 18 a that the active compartment population increases immediately because $\alpha(t)$ is increased. In Fig. 18 b it is seen that the resting compartment decreases drastically because it must send additional cells to both the active compartment and the maturation compartment. The transient peaks in it are the result of cell influxes from the active state. Fig. 18 c shows that the maturation population is the first compartment to detect the

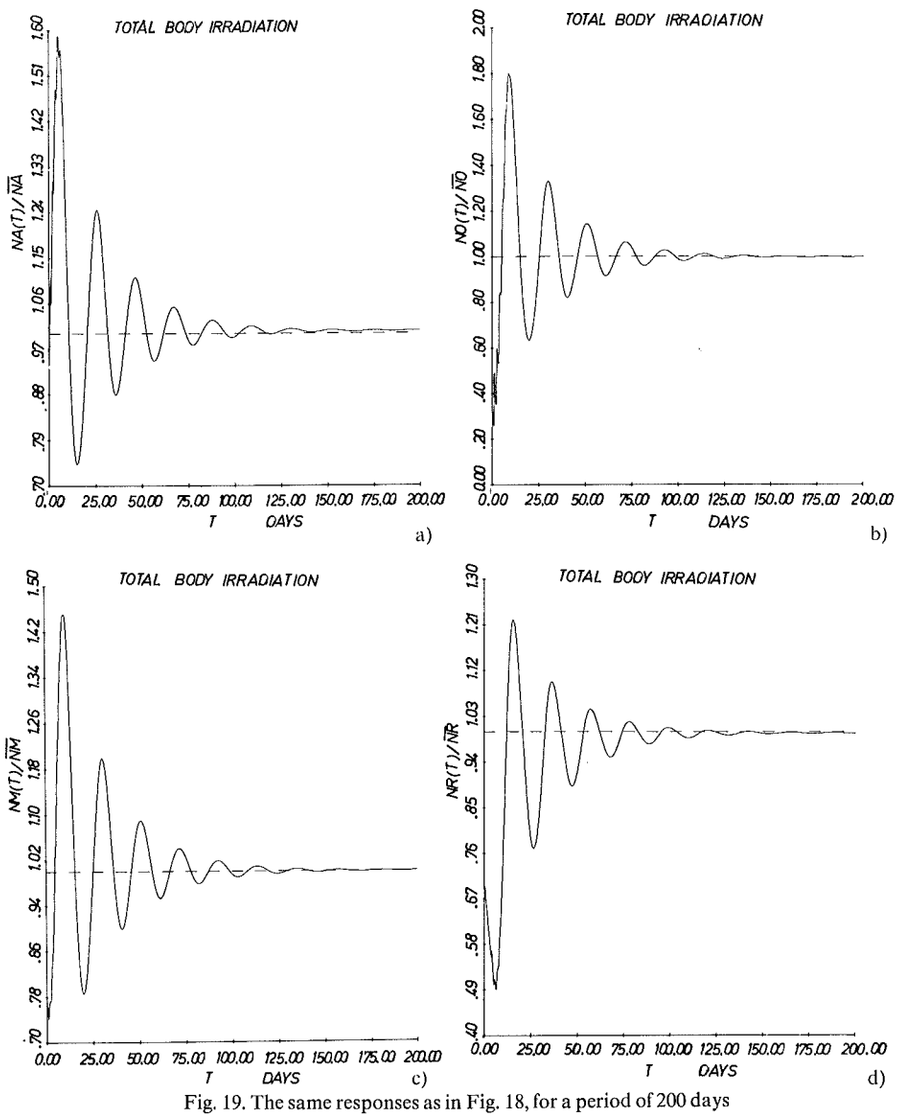

Fig. 19. The same responses as in Fig. 18, for a period of 200 days

increase in population due to the increased proliferation rate, after about 4 days. Fig. 18 d shows that the reserve compartment does not share in this population increase because of the demands made on it by the blood compartment.

In Figs. 19 a—19 d we see the long term behavior of these same populations over a period of 200 days. These curves indicate that the long term small amplitude oscillatory behavior of the blood cell population is likewise a feature

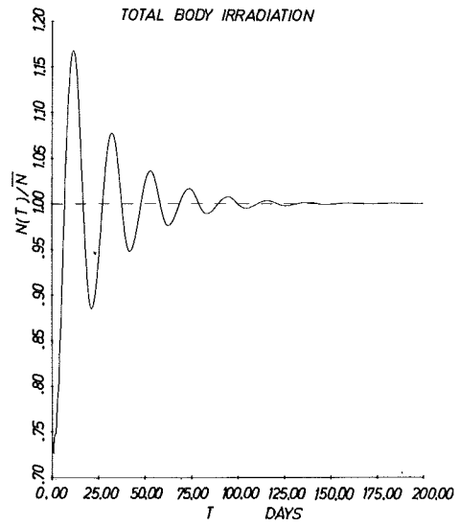

Fig. 20. The theoretical dependence of the total normalized neutrophil population $N(t)/\bar{N}$ on the time t following a total body elimination of 25% of the population, uniformly in each compartment, at $t=0$. Parameter values are as for Fig. 16

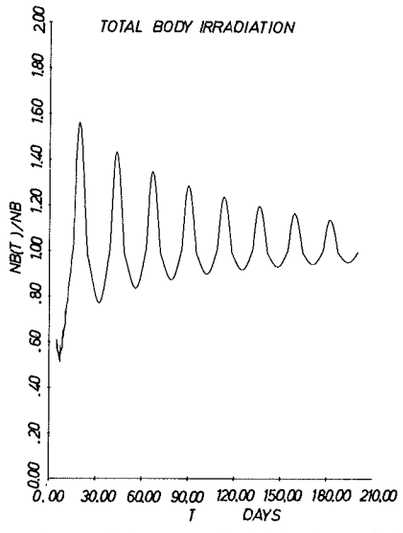

Fig. 21. The theoretical dependence of the normalized blood population $N_B(t)/\bar{N}_B$ on the time t, in response to an elimination of 50% of the total neutrophil population, uniformly in each compartment. The parameter values are the same as for Fig. 16, with the exception that $1/\gamma_0=96$ hr

of every compartment. It is noteworthy that it takes a long time, approximately 15 days, for the reserve compartment to first achieve its steady state value, as is seen in Fig. 19 c. This is a much longer time interval than is needed by any of the other compartments. Such an inference is also suggested by the shielded hindlimb irradiation experiments in mice, quoted in Figs. 5—7. In Fig. 20 is shown a plot of the total normalized neutrophil population $N(t)/\bar{N}$. The long-term behavior of the normalized blood population in response to a theoretical total body depletion of 50% is shown in Fig. 21. In contrast to the curve of Fig. 17 b corresponding to an initial depletion of 25%, the long term oscillations are of greater amplitude and decay more slow.

8. Conclusions

A mathematical model of the total neutrophil production system has been introduced which consists of five compartments, an active compartment and a resting compartment which comprise the proliferative pool, and maturation, reserve, and blood compartments comprising the nonproliferative pool. These appear to be the minimum number of compartments necessary to simulate the principal features of the neutrophil system. The nonlinear control elements which are introduced regulate homeostatically the total number of neutrophils in the blood and the total number of cells characterizing the system. The model contains 13 parameters in its simplest formulation, of which 7 can be characterized as steady state parameters, and 6 can be characterized as dynamical parameters which determine the dynamical response of the system to perturbations. Because there is so little quantitative information regarding the dynamical response of the system, these parameters are for the most part arbitrary, with the exception of perhaps two of them.

We have solved our model equations for various initial conditions, so as to represent different experimental observations that have been made in the past of the neutrophil production system. We find that we are able to reproduce the known behavior of the neutrophil production system in a comprehensive manner, with an appropriate choice of the values of the parameters. Most of the values we inferred for the steady state parameters and other quantitative properties of the system are not qualitatively different from those made by one or another investigator. Rather, we stress that what is novel is the comprehensive and quantitative nature of our model. By simulating most of the experimental facts, we impose contraints of consistency upon the inferences made about the entire system that are not revealed in the examination of the production system in a piece-wise fashion. Thus, we find that there is little leeway in the determination of most of the steady state parameters.

The dynamical aspect of our model are somewhat new. The most notable feature of the dynamical response of the system to large perturbations in the number of blood cells or in the total number of cells of the production system is that the system "rings", displaying an oscillatory behavior in the number of cells in the blood and other compartments of the system, as a function of the time. Such large

perturbations are produced by leukopheresis or exposure of the system to disease, which deplete the number of blood cells, and in total body irradiation experiments or some drug treatments, wich deplete the total number of cells in the production system. However, the calculated amplitude of oscillation is rather small, and the oscillation is damped, which may explain why the reports of such oscillations in the blood of some apparently normal individuals are rare. Their natural occurrence, of course, would require a large initial perturbation of the system, or a significant alteration of some of the normal steady state parameters of the systems. Such an alteration presumably occurs in the disease state cyclic neutropenia.

This work has been supported in part by the National Cancer Institute, grant no. NCI R-5ROICA-12124-03.

Appendix

Here we follow the method of calculation introduced by Rubinow [5]. We assign a cell density function n_i to each compartment i with the notation $i=1$ for myeloblasts, $i=2$ for promyelocytes, $i=3$ for myelocytes, and $i=4$ for metamyelocytes. In the steady state, n_i is constant within each compartment. The mean generation time in each compartment is denoted by T_i, $i=1, 2, 3, 4$. The total population N_i in the i-th compartment is given by the formula

$$N_i=n_i\, T_i, \qquad i=1, 2, 3, 4. \tag{A 1}$$

The transition from one compartment to the next is assumed to be proceeded by cell division. Let r_i denote the fraction of daughter cells of the i-th compartment which are of the same type as their parents. Then $r_i=1$ means that all the daughters are of the same type as their parent. $r_i=0$ means that all the daughters are of the succeeding cell type. A value of r_i between these two extremes represents the condition that cell division produces a mixture of these two outcomes. Such a condition can arise because cell division is asymmetric in its outcome, or because there are two different outcomes of cell division. For example, a myelocyte may first divide to form two daughter myelocytes, and the daughters (with the same mean generation time as the parent) then divide to produce two metamyelocytes. We shall, for simplicity, assume here that all cells in a compartment i undergo division after a time T_i spent in the compartment, following birth. Then, as shown in reference 5, the following equations representing conservation of cell flux relate the various compartments:

$$\begin{aligned} n_1\,(1-2\,r_1)&=s_0, \qquad n_2\,(1-2\,r_2)=s_0+n_1,\\ n_3\,(1-2\,r_3)&=s_0+n_1+n_2, \qquad n_4=s_0+n_1+n_2+n_3. \end{aligned} \tag{A 2}$$

Here, s_0 is the hypothetical (constant) stem cell flux into the myeloblast compartment. We note here that n_i also represents the cell production rate in the i-th compartment.

In this model, the mitotic index f_{Mi}, the fraction of cells in the i-th compartment in mitosis, is expressed simply as the ratio of the mitotic time T_{Mi} to the generation time T_i, or,

$$f_{Mi}=\frac{T_{Mi}}{T_i},\quad i=1,2,3. \tag{A 3}$$

Similarly, the labeling index f_{Li}, in the i-th compartment, the fraction of cells in S-phase (which is labeled with tritiated thymidine following a pulse exposure), is expressed in terms of the S-phase duration T_{Si} as

$$f_{Li}=\frac{T_{Si}}{T_i},\quad i=1,2,3. \tag{A 4}$$

In reference 5, we assumed that $s_0=0$, $T_{M1}=T_{M2}=T_{M3}$, while f_{Mi} and N_i were as given by Killman et al. [53] (see Tables 1 and 2). It was inferred there that $(r_1, r_2, r_3)=(.50, .75, .71)$, $(T_1, T_2, T_3)=(25, 42, 57)$ hr, and $T_{M1}=0.62$ hr. The inferred generation times are in excellent agreement with the observed [19] grain-count halving times $(T_1, T_2, T_3)=(31, 24\text{—}60, 54\text{—}58)$ hr. The derived labeling indices, assuming $T_{S1}=T_{S2}=T_{S3}=15$ hr, become $(f_{L1}, f_{L2}, f_{L3})=(.60, .36, .26)$. These values are perhaps in tolerable agreement with observation, as shown in Table 3. However, the inferred mitotic times are not in agreement with the direct observations of average mitotic times of Rondanelli et al. [54]: $(T_{M1}, T_{M2}, T_{M3})=(0.75, 0.90. 1.07)$ hr. It is seen that the mitotic times in the proliferative compartments are unequal, and their average is 0.91 hr.

Let us apply equations (A 1 – A 3) to the extensive data of Rondanelli et al. [54] concerning mitotic indices. These indices, quoted in Table 2, were obtained by counting 10,000 marrow proliferative cells in each of 10 normal donors. These investigators also found that $(N_1, N_2, N_3)=(1, 2.15, 9.15)$, where N_1 has been arbitrarily chosen to be unity. Under the assumption that the stem cell flux ratio s_0 is negligible, it is readily found that $r_1=\frac{1}{2}$, $r_2\approx r_3\approx 0$, and $(T_1, T_2, T_3)=(32, 68, 135)$ hr. Assuming now that $T_{S1}=T_{S2}=T_{S3}=15$ hr we infer that labeling indices should be $(f_{L1}, f_{L2}, f_{L3})=(.47, .22, .11)$. While the labeling index for the myeloblast is perhaps in tolerable agreement with observations, the labeling indices for the promyelocytes and myelocytes are not. Also, the generation time assigned to myelocytes appears to be too large. Hence, the mitotic index data of Rondanelli et al., on the basis of the above model, is not consistent with either the labeling index data, or the generally accepted generation time estimates for myelocytes.

Cronkite and Vincent [3], in their model of steady state proliferation, assumed that the proliferative pool consisted of a sequence of subpools, each with the property that cell division in one subpool produced two new cells of the next subpool type. They also assumed that $s_0\neq 0$, one subpool each makes up the myeloblast and promyelocyte compartments, and that the myelocyte compartment consists of two subpools. They accepted, for the values of N_i, the data of Cronkite et al. [55] (see Table 1).

We shall utilize the present formalism in order to reproduce the results of their calculation, and to draw some further inferences. To do so, identify $i=1$ as the

myeloblast compartment, $i=2$ as the promyelocyte compartment, and $i=3$ plus $i=4$ as the myelocyte compartment. Thus, the total number of myelocytes is

$$N_3+N_4=n_3\ T_3+n_4\ T_4. \tag{A 5}$$

The assumption of serial division requires that $r_i=0$ in equations (A 2), $i=1, 2, 3$. These authors further assumed that $T_3=T_4$. and accepted for the experimentally determined values of the labeling index and S-phase interval in the myelocyte compartment, 0.234 and 12 hr respectively. Thus, with

$$f_{L3}=\frac{(n_3+n_4)\ T_{S3}}{N_3+N_4}=\frac{T_{S3}}{T_3}, \tag{A 6}$$

it is immediately inferred that $T_3=51.3$ hr. We make use of equations (A 1—A 3) with $r_i=0$, and the assumed values of the relative number of cells in each proliferative compartment, with N_1 arbitrarily set equal to 100 cells. It is readily found that

$$(s_0, n_1, n_2, n_3+n_4)=(7.64, 7.64, 15.3, 9.17)\ \mathrm{hr}^{-1}, \tag{A 7}$$

and that the efflux rate to the metamylecyte compartment $n_5=2\,n_4=122$/hr.

As Cronkite and Vincent indicated, the latter value is close to the observed number of cells entering the metamyelocyte compartment of 147 cells/hr/100 myeloblasts. Furthermore, it is found, assuming the labeling indices are as given by Cronkite et al. [55], that $T_{S1}=11.1$ hr, and $T_{S2}=12.4$ hr. Hence, the DNA synthesis time is virtually the same in all compartments, which is perhaps an appealing conclusion. However, as these authors also point out, with $s_0=$ 7.6 cells/hr/100 myeloblasts, if the value of T_S in stem cells is 12 hr, there would be 91 labeled stem cells/85 labeled myeloblasts following flash labeling, and "one must wonder why a cell in this apparent abundance is not recognized". The authors of this model do not comment on the fact that the inferred values of T_1 and T_2 are 13.1 hr, and 19.0 hr, respectively. These values are in glaring disagreement with the observed grain-count halving estimates for these generation times [19]. Furthermore, accepting the Rondanelli et al. [54] values of the mitotic indices, it is inferred with the aid of equation (43) that the mitotic times $(T_{M1}, T_{M2}, T_{M3})=(0.31, 0.25, 0.41)$ hr. These, too, are in serious disagreement with the observations of mitotic times quoted previously [54].

We conclude that the present day estimates of the kinetic parameters of the proliferative neutrophil precursor pools are not consistent with any given theoretical scheme of proliferation.

Acknowledgement

We thank Dr. David W. Alling for his useful comments on the original manuscript.

References

[1] Cartwright, G. E., Athens, J. W., Boggs, D. R., Wintrobe, M. M.: The Kinetics of Granulopoiesis in Normal Man. Series Haemat. *1*, 1 (1965).
[2] Boggs, D. R.: Leukopoiesis. Ann. Rev. Physiol. *28*, 39 (1966); The Kinetics of Neutrophilic Leukocytes in Health and in Disease. Sem. Hemat. *4*, 359 (1967).
[3] Cronkite, E. P., Vincent, P. C.: Granulocytopoiesis. Ser. Haemat. *2*, 3 (1969).
[4] Perry, S.: Proliferation of Myeloid Cells. Ann. Rev. Med. *22*, 171 (1971).

[5] Rubinow, S. I.: A Simple Model of a Steady State Differentiating Cell System. J. Cell Biol. *43*, 32 (1969).
[6] Warner, H. R., Athens, J. W.: An Analysis of Granulocyte Kinetics in Blood and Bone Marrow. Ann. N. Y. Acad. Sci. *113*, 523 (1964).
[7] King-Smith, E. A., Morley, A.: Computer Simulation of Granulopoiesis: Normal and Impaired Granulopoiesis. Blood *36*, 254 (1970).
[8] Harris, P. F., Harris, R. S., Kugler, J. H.: Studies of the Leucocyte Compartment in Guinea-Pig Bone Marrow after Acute Haemorrhage and Severe Hypoxia: Evidence for a Common Stem-Cell. Brit. J. Haemat. *12*, 419 (1966).
[9] Lawrence, J. S., Craddock, C. G., Jr.: Stem Cell Competition: The response to antineutrophilic serum as affected by hemorrhage. J. Lab. Clin. Med. *72*, 731 (1968).
[10] Till, J. E., McCulloch, E. A.: A Direct Measurement of the Radiation Sensitivity of Normal Mouse Bone Marrow Cells. Radiat. Res. *14*, 213 (1961).
[11] van Bekkum, D. W., van Noord, M. J., Maat, B., Dicke, K. A.: Attempts at Identification of Hemopoietic Stem Cell in Mouse. Blood *38*, 547 (1971).
[12] Bainton, D. R., Farquhar, M. G.: Origin of Granules in Polymorphonuclear Leukocytes. J. Cell Biol. *28*, 277 (1966).
[13] Athens, J. W., Raab, S. O., Haab, O. P., Mauer, A. M., Ashenbrucker, H., Cartwright, G. E., Wintrobe, M. M.: Leukokinetic Studies, III. The Distribution of Granulocytes in the Blood of Normal Subjects. J. Clin. Invest. *40*, 159 (1961).
[14] Athens, J. W., Haab, O. P., Raab, S. O., Mauer, A. M., Ashenbrucker, H., Cartwright, G., E., Wintrobe, M. M.: Leukokinetic Studies, IV. The Total Blood, Circulating and Marginal Granulocyte Pools and the Turnover Rate in Normal Subjects. J. Clin. Invest. *40*, 989 (1961).
[15] Fliedner, T. M., Cronkite, E. P., Robertson, J. S.: Granulocytopoiesis. I. Senescence and Random Loss of Neutrophilic Granulocytes in Human Beings. Blood *24*, 402 (1964).
[16] Killman, S. A.: Acute Leukemia: The Kinetics of Leukemic Blast Cells in Man. Ser. Haemat. *1*, 3, 38 (1968).
[17] Stryckmans, P., Cronkite, E. P., Fache, J., Fliedner, T. M., Ramos, J.: Deoxyribonucleic Acid Synthesis Time of Erythropoietic and Granulopoietic Cells in Human Beings. Nature *211*, 717 (1966).
[18] Todo, A.: Proliferation and differentiation of hematopoietic cells in hematologic disorders. 3. In vivo radioautographic study of leukemia including erythroleukemia. Acta. Haemat. Japan. *31*, 947 (1968).
[19] Cronkite, E. P., Bond, V. P., Fliedner, T. M., Killman, S. A.: The Use of Tritiated Thymidine in the Study of Hemopoietic Cell Proliferation, in: Ciba Foundation Symposium on Haemopoiesis Wolstenholme, G. E. W., O'Connor, M., eds.), p. 70. London: Churchill 1960.
[20] Killman, S. A., Cronkite, E. P., Fliedner, T. M., Bond, V. P.: Mitotic Indices of Human Bone Marrow Cells. III. Duration of Some Phases of Erythrocyte and Granulocytic Proliferation Computed from Mitotic Indices. Blood *24*, 267 (1964).
[21] Boll, I., Kuhn, A.: Granulocytopoiesis in Human Bone Marrow Cultures Studies by Means of Kinematography. Blood *26*, 449 (1965).
[22] Perry, S., Moxley, J. H., III, Weiss, G. H., Zelen, M.: Studies of Leukocyte Kinetics by Liquid Scintillation Counting in Normal Individuals and in Patients with Chronic Myelocytic Leukemia. J. Clin. Invest. *45*, 1388 (1966).
[23] Cartwright, G. E., Athens, J. W., Wintrobe, M. M.: The Kinetics of Granulopoiesis in Normal Man. Blood *24*, 780 (1964).
[24] Perry, S., Craddock, C. G., Jr., Lawrence, J. S.: Rates of Appearance and Disappearance of White Blood Cells in Normal and in Various Disease States. J. Lab. Clin. Med. *51*, 501 (1958).
[25] Bond, V. P., Fliedner, T. M., Cronkite, E. P., Rubini, J. R., Robertson, J. S.: Cell Turnover in Blood and Blood-Forming Tissues Studied with Tritiated Thymidine, in: Kinetics of Cellular Proliferation (Stohlman, F., Jr., ed.), p. 188. New York: Grune and Stratton 1969.
[26] Donohue, D. M., Reiff, R. H., Hansen, M. L., Belson, Y., Finch, C. A.: Quantitative Measurement of the Erythrocytic and Granulocytic Cells of the Marrow and Blood. J. Clin. Invest. *37*, 1571 (1958).
[27] Craddock, C. G., Jr., Perry, S., Lawrence, J. S.: The Dynamics of Leukopoiesis and Leukocytosis, as Studied by Leukophereis and Isotopic Techniques. J. Clin. Invest. *35*, 285 (1956).

[28] Patt, H. M., Maloney, M. A., Jackson, E. M.: Recovery of Blood Neutrophils after Acute Peripheral Depletion. Amer. J. Physiol. *188*, 585 (1957).
[29] Bierman, H. R., Kelly, K. H., Byron, R. L., Jr., Marshall, G. J.: Leucapheresis in Man I. Haematological Observations Following Leucocyte Withdrawal in Patients with Non-Haematological Disorders. Brit. J. Haemat. *7*, 51 (1961).
[30] Boggs, D. R., Athens, J. W., Cartwright, G. E., Wintrobe, M. M.: Leukokinetic Studies. IX. Experimental Evaluation of a Model of Granulopoiesis. J. Clin. Invest. *44*, 643 (1965).
[31] Dornfest, B. S., LoBue, J., Handler, E. S., Gordon, A. S., Quastler, H.: Mechanisms of Leukocyte Production and Release. II. Factors Influencing Leukocyte Release from Isolated Perfused Rat Legs. J. Lab. Clin. Med. *60*, 777 (1962).
[32] Gordon, A. S., Handler, E. S., Siegel, C. O., Dornfest, B. S., LoBue, J.: Plasma Factors Influencing Leukocyte Release in Rats. Ann. N. Y. Acad. Sci. *113*, 766 (1964).
[33] Boggs, D. R., Cartwright, G. E., Wintrobe, M. M.: Neutrophilia-Inducing Activity in Plasma of Dogs Recovering from Drug-Induced Myelotoxicity. Amer. J. Physiol. *211*, 51 (1966).
[34] Marsh, J. C., Boggs, D. R., Cartwright, G. E., Wintrobe, M. M.: Neutrophil Kinetics in Acute Infection. J. Clin. Invest. *46*, 1943 (1967).
[35] Athens, J. W., Haab, A. P., Raab, S. O., Boggs, D. R., Ashenbrucker, H., Cartwright, G. E., Wintrobe, M. M.: Leukokinetic Studies. X. Blood Granulocyte Kinetics in Chronic Myelocytic Leukemia. J. Clin. Invest. *44*, 778 (1965).
[36] Galbraith, P. R., Valberg, L. S., Brown, M.: Patterns of Granulocyte Kinetics in Health, Infection, and in Carcinoma. Blood *25*, 683 (1965).
[37] Vogel, J. M., Yankee, R. A., Kimball, H. R., Wolff, S. M., Perry, S.: The Effect of Etiocholanolone on Granulocyte Kinetics. Blood *30*, 474 (1967).
[38] Lajtha, L. G., Gilbert, C. W., Porteous, D. D., Alexanian, R.: Kinetics of A Bone-Marrow Stem-Cell Population. Ann. N. Y. Acad. Sci. *113*, 742 (1964).
[39] Morley, A., Stohlman, F., Jr.: Studies on the Regulation of Granulopoiesis. I. The Response to Neutropenia. Blood *35*, 312 (1970).
[40] Morley, A., Rickard, K. A., Howard, D., Stohlman, F., Jr.: Studies in the Regulation of Granulopoiesis. IV. Possible Hemoral Regulation. Blood *37*, 14 (1971).
[41] Rytomaa, T., Kiviniemi, K.: Control of Granulocyte Production. I. Chalone and Antichalone, Two Specific Hemoral Regulators. Cell Tissue Kinet. *1*, 329 (1968).
[42] Morley, A. A.: A Neutrophil Cycle In Healthy Individuals. Lancet *2*, 1220 (1966).
[43] Dale, D. C., Alling, D. W., Wolff, S. M.: Application of Time Series Analysis to Serial Blood Neutrophil Counts in Normal Individuals and Patients Receiving Cyclophosphamide. Brit. J. Haemat. *24*, 57 (1973).
[44] King-Smith, E. A., Morley, A.: Computer Simulation of Granulopoiesis; Normal and Impaired Granulopoiesis. Blood *36*, 254 (1970).
[45] Morley, A. A., Baikie, A. G., Galton, D. A. G.: Cyclic Leucocytosis as Evidence for Retention of Normal Homeostatic Control in Chronic Granulocytic Leukemia. Lancet *2*, 1320 (1967).
[46] Guerry, IV, D., Dale, D. C., Omine, M., Perry, S., Wolff, S. M.: Periodic Hematopoiesis in Human Cyclic Neutropenia. J. Clin. Invest. *52*, 3220 (1973).
[47] Osgood, E. E., Seaman, A. J.: The Cellular Composition of Normal Bone Marrow as Obtained by Sternal Puncture. Physiol. Rev. *24*, 46 (1944).
[48] Vaughan, S. L., Brockmyre, F.: Normal Bone Marrow as Obtained by Sternal Puncture. Blood *1 S*, 54 (1947).
[49] Miale, J. B.: Laboratory Medicine-Hematology, 3rd ed. St. Louis: Mosby 1967.
[50] Wintrobe, M. M.: Clinical Hematology, 6th ed. Philadelphia: Lea and Febiger 1967.
[51] Athens, J. W.: Neutrophilic Granulocyte Kinetics and Granulocytopoiesis, in: Regulation of Hematopoesis (Gordon, A. S., ed.), Vol. 2, p. 1143. New York: Appleton Century-Crofts 1970.
[52] Lala, P. K., Maloney, M. A., Patt, H. M.: A Comparison of Two Markers of Cell Proliferation in Bone Marrow. Acta Haemat. *31*, 1 (1964).
[53] Killman, S. A., Cronkite, E. P., Fliedner, T. M., Bond, V. P.: Mitotic Indices of Human Bone Marrow Cells. I. Number and Cytologic Distribution of Mitoses. Blood *19*, 743 (1962).
[54] Rondanelli, E. G., Magliulo, E., Giraldi, A., Carco, F. P.: The Chronology of the Mitotic Cycle of Human Granulocytopoietic Cells. Blood *30*, 557 (1967).
[55] Cronkite, E. P., Fliedner, T. M., Stryckmans, P., Chanana, A. D., Cuttner, J., Ramos, J.: Flow Patterns and Rates of Human Erythropoiesis and Granulocytopoiesis. Ser. Haemat. *5*, 51 (1965).

[56] Videbaek, A.: Normal bone marrow punctates from individuals in various age groups. Folia haemat. *65*, 203 (1941).
[57] Begemann, H., Hemmerle, W.: Die Mitosetätigkeit des menschlichen Knochenmarks und ihre Beeinflussung durch cytostatische Substanzen. Klin. Wschr. *27*, 530 (1949).
[58] Boll, I., Ganssen, O.: Die Mitosedauer der Paraleukoblasten. Acta haemat. *27*, 229 (1962).
[59] Lundmark, K. M.: Bone Marrow Cell Proliferation in Health and in Haematological Disease During Childhood. Acta paediat. (Uppsala), Suppl. *162*, 6 (1966).
[60] Gavosto, F.: Nucleic Acids and Protein Metabolism of Bone Marrow Cells Studied by Means of Tritium-Labelled Precursors, in: Tritium in the Physical and Biological Sciences. Vol. 2, p. 237. Vienna: Intern. Atomic Energy Agency 1962.
[61] Mauri, C., Torelli, U., Artusi, T., Grossi, G., Emilia, G.: Autoradiographische Untersuchungen über den RNS- und Proteinstoffwechsel der unreifen Zellen bei akuter Leukämie. Vorläufige Mitteilung. Schweiz. Med. Wschr. *95*, 1485 (1965).
[62] Kuroyanagi, T., Saito, M.: Proliferative capacity of leukemic cells studied with tritiated thymidine in vitro. Tohoko J. exp. Med. *80*, 168 (1962).
[63] Mauri, C.: DNA synthesis and mitotic rate in leukaemic cells. Cancro *15*, 145 (1962).
[64] Lin, M. S., Bouroncle, B. A.: The Size and Transit Time of Nondividing Subpool of Precursor Cells in Acute Leukemia. Blood *29*, 63, (1967).
[65] Alfrey, C. P., Jr., Kiely, J. M., Tauxe, W. N., Owen, C. A., Jr.: In Vitro DNA Synthesis by Human Marrow Cells. Blood *18*, 794 (1961).
[66] Schmid, J. R., Kiely, J. M., Tauxe, W. N., Owen, C. A., Jr.: In Vitro DNA and RNA Synthesis in Human Bone Marrow Cells: A Study of 12 Normal Subjects and 12 Patients with Lymphoplasmocytic Disorders. Blood *27*, 310 (1966).
[67] Ogawa, M.: H^3-thymidine Autoradiograph. Studies of Cellular Proliferation in Acute Leukemia Using H^3-thymidine. Nagoya Med. Assn. J. *90*, 91 (1967).
[68] Scherbaum, O., Rasch, G.: Cell Size Distribution and Single Cell Growth in Tetrahymena Pyriformis GL. Acta Pathol. Microbiol. Scand. *41*, 161 (1957).
[69] von Foerster, H.: Some Remarks on Changing Populations, in: The Kinetics of Cellular Proliferation (Stohlman, F., Jr., ed.), p. 382. New York: Grune and Stratton (1959).

S. I. Rubinow and J. L. Lebowitz
Biomathematics Division
Graduate School of Medical Sciences
Cornell University
New York, NY 10021, U.S.A.

Printed in Austria
Druck: Paul Gerin, A-1021 Wien